

**JIMMA UNIVERSITY**  
**SCHOOL OF GRADUATE STUDIES**  
**COLLEGE OF NATURAL SCIENCES**  
**DEPARTMENT OF CHEMISTRY**



**SYNTHESIS OF NICKEL OXIDE NANOPARTICLES AND COPPER DOPED NICKEL OXIDE NANOCOMPOSITES USING *PHYTOLACCA DODECANDRA L'HERIT* LEAF EXTRACT AND EVALUATION OF ITS ANTIOXIDANT AND PHOTOCATALYTIC ACTIVITIES.**

**BY: SORUMA GUDINA**

**ADVISOR**

**GUTA GONFA (PhD)**

**CO-ADVISOR**

**AHMAD AWOL (Ass. prof)**

**NOVEMBER, 2021**

**JIMMA, ETHIOPIA**

SYNTHESIS OF NICKEL OXIDE NANOPARTICLES AND COPPER DOPED NICKEL OXIDE NANOCOMPOSITES USING *PHYTOLACCA DODECANDRA L'HERIT* LEAF EXTRACT AND EVALUATION OF ITS ANTIOXIDANT AND PHOTO CATALYTIC ACTIVITIES.

A THESIS SUBMITTED TO THE SCHOOL OF GRADUATE STUDIES OF JIMMA UNIVERSITY IN PARTIAL FULFILMENT OF THE REQUIREMENTS FOR THE DEGREE OF MASTERS OF SCIENCE IN CHEMISTRY (INORGANIC CHEMISTRY)

**BY: SORUMA GUDINA**

ADVISOR

**GUTA GONFA (PhD)**

CO-ADVISOR

**AHMAD AWOL (Asst. prof)**

## **Declaration**

I declare that the work described in this thesis is my original work under the supervision of my advisors, Dr. Guta Gonfa (PhD) and Mr. Ahmad Awol (Asst. prof) at the Department of Chemistry, Jimma University for the degree of M.Sc. in Inorganic Chemistry.

I also declare that the substance of this thesis has neither been submitted elsewhere nor is being currently submitted for any other degree.

I further declare that the thesis embodies the results of my research or advanced studies and that it has been composed by me. Where appropriate I had acknowledged the work of others.

Name: Soruma Gudina

Signature: \_\_\_\_\_

Place: Jimma University, Jimma.

### Graduate Thesis Ownership Agreement

This thesis is a property of Jimma University, an institution that awarded MSc/PhD Degree to the graduate student and funded its research cost fully or partly. The research work was accomplished under the close support and supervision of the assigned University's academic staff. It is therefore strictly forbidden to publish, modify, or communicate to or put at the disposal of third party the entire document or any part thereof without the common consent of the research supervisor(s) and the graduate student. Disregarding this agreement would lead to accountability according to the Jimma University's Research and Publication Misconduct Policy **Article 1.7** of the University's Document for "Guidelines and Procedures for Research, March 2012".

Name of the Graduate Student

Signature

Date

---

---

---

Name (s) of the Research Supervisor (s)

Signature

Date

---

---

---

---

---

---

Title of the Thesis:

---

---

Degree Awarded: MSc/PhD (Encircle one)

College of Natural Sciences, Jimma University

SCHOOL OF GRADUATE STUDIES  
JIMMA UNIVERSITY  
COLLEGE OF NATURAL SCIENCES  
MSc THESIS APPROVAL SHEET

We, the undersigned, member of the Board of Examiners of the final open defense by Sonam Gudim have read and evaluated his thesis entitled "Synthesis of nickel oxide nanoparticles and Copper doped Nickel oxide nanocomposites using *Phytolacca dodecandra* L'herit Leaf extract and evaluation of its antioxidant and photocatalytic activities.." This is therefore to certify that the *thesis* has been accepted in partial fulfillment of the requirements for the degree master of Science in Chemistry (Inorganic)

Name of the Chairperson	Signature	Date
<u>Gutta Gonfa(PhD)</u>		
Name of Major Advisor	Signature	Date
<u>Kirubel Teshome (Assist. Prof.)</u>		<u>Nov 27, 2021</u>
Name of the Internal Examiner	Signature	Date
<u>Raji Feyisa(PhD)</u>		
Name of the External Examiner	Signature	Date

SCHOOL OF GRADUATE STUDIES  
JIMMA UNIVERSITY  
COLLEGE OF NATURAL SCIENCES  
PERFORMANCE CERTIFICATE FOR MASTER'S DEGREE

Name of student: Soruma Gudina ID No. \_\_\_\_\_  
Graduate Program: Regular Msc

Course Code	Course Title	Cr. Hr	Number Grade	Rank**	Remark
	MSc Thesis				

\*\*Excellent, Very Good, Good, Satisfaction, Fail

Thesis Title:  
Synthesis of nickel oxide nanoparticles and Copper doped Nickel oxide nanocomposites using *Phytolacca dodecandra L'herit* Leaf extract and evaluation of its antioxidant and photocatalytic activities.

Board of Examiner's decision Mark X in one of the boxes. Pass  Failed

If failed, give reasons and indicate plans for re-examination.

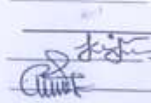
3. Approved by: Name and Signature of members of the examining Board, and Department Head

Chairman \_\_\_\_\_

External Examiner: Raji Feyisa(PhD)

Internal Examiner: Kirubel Teshome (Ass. Prof.)

Major Advisor: Gutta Gonfa (PhD)



Nov 27, 2021

\_\_\_\_\_  
Department Head

\_\_\_\_\_  
Signature

\_\_\_\_\_  
Date

## TABLE OF CONTENTS

CONTENTS	PAGE
LIST OF TABLES.....	x
LIST OF ABBREVIATIONS AND ACRONYMS.....	xi
ACKNOWLEDGMENT.....	xii
ABSTRACT.....	xiii
1. INTRODUCTION .....	1
1.1 Background of the study .....	1
1.2 Statement of the problems.....	3
1.3 Objectives of the study.....	4
1.3.1 General objective .....	4
1.3.2 Specific objectives .....	4
1.4 The Significance of the study.....	4
2. LITERATURE REVIEW .....	6
2.1 Nanoparticles .....	6
2.2 Green synthesis .....	9
2.2.1 Mechanism of Green Synthesis.....	10
2.2.2 <i>Phytolacca dodecandra l'herit</i> .....	11
2.3 Characterization technique for metal and metal oxide nanoparticles .....	15
2.3.1 UV-Vis spectroscopy .....	15
2.3.2 Fourier Transformation Infrared (FT-IR) Spectroscopy .....	15
2.3.3 X-ray diffraction (XRD) .....	16
2.3.4 Scanning electron microscopy (SEM) .....	16
2.4. Dyes .....	17
2.5. Antioxidant. ....	21
3. MATERIALS AND METHODS .....	23
3.1. The study area and period .....	23
3.1.1. Materials .....	23
3.1.2. Chemicals.....	23
3.1.3. Apparatus and equipment.....	23
3.2. Sample collection and preparation.....	23
3.3. Phytochemical test of <i>phytolacca dodecandra l'herit</i> leaves extract.....	24

3.3.1. Test for flavonoids .....	24
3.3.2. Test for alkaloids.....	24
3.3.3. Test for saponins .....	24
3.3.4. Test for tannins and phenolic compounds.....	24
3.4. Synthesis of nickel oxide nanoparticles .....	24
3.5. Synthesis of copper doped nickel oxide nanocomposites .....	24
3.6. Physicochemical Methods of Characterization.....	25
3.7. Photocatalytic degradation of dye.....	26
3.8. Antioxidant Activity .....	26
4. RESULTS AND DISCUSSIONS.....	27
4.1. Phytochemical analysis of <i>Phytolacca dodecandra l'herit</i> leaves extract .....	27
4.2. Synthesis. ....	28
4.2.1 Synthesis of NiO NPs .....	28
4.2.2. Synthesis Cu-NiO NCs .....	28
4.2.3. Optimization of different parameters. ....	28
4.3. Characterization of the synthesized samples.....	30
4.3.1. Electronic spectra of the synthesized nanoparticles.....	31
4.3.2. Fourier transform infrared (FT-IR) spectroscopy .....	32
4.3.3. X-ray diffraction (XRD) analysis.....	35
4.3.4. Scanning Electron Microscopy (SEM) analysis .....	36
4.4. Photocatalytic Degradation of Dye .....	38
4.4.1. Effect of pH of the solution.....	38
4.4.2. Effect of initial dye concentration.....	40
4.4.3. Effect of irradiation time.....	41
4.4.4. Effect of catalyst dose.....	41
4.4.5. Reusable performance of the nanoparticles. ....	42
4.5. Antioxidant activity .....	43
5. CONCLUSION AND RECOMMENDATION .....	45
5.1. Conclusion .....	45
5.2. Recommendation .....	45
6. REFERENCES.....	46
APPENDIX.....	54



## LIST OF FIGURES

FIGURES	PAGE
Figure 1. Graphics Abstract of the synthesized NPs using <i>Phytolacca dodecandra l'herit</i> leaf...xiv	
Figure 2.The schematic representation of the top-down and bottom-up approaches for the production of metal oxide nanostructures.....	8
Figure 3. Different methods for synthesizing nanoparticles.....	9
Figure 4. Chemical structure of Steroid (dexamethasone) (A) and phenolic acid (B) .....	10
Figure 5. Graphics Abstract of Preparation of nickel oxide nanoparticles using <i>Aegle marmelos</i> leaves.....	11
Figure 6. <i>Phytolaccadodecandra l'herit</i> plant .....	12
Figure 7. Structure of phenolic compounds.....	13
Figure 8. Structures of alkaloids: (a) morphine and (b) atropine.....	13
Figure 9. Structures of (A) triterpenoid and (B) steroidal saponins .....	14
Figure 10. Flavonoids subgroup structure. ....	14
Figure 11. The Pollutant and affected water body by organic dyes.....	18
Figure 12. Photocatalytic degradation mechanism of CR over NPs.....	19
Figure 13. Photocatalytic degradation mechanism of Methylene blue (MB) dye by the green-synthesized Al-MnO NAPs using leaf extract of <i>Abutilon indicum</i> under visible ligh. ....	20
Figure 14. Scheme of Illustration of catalytic properties of Au NPs in decomposing H <sub>2</sub> O <sub>2</sub> .....	21
Figure 15. Results of the Phytochemical test of <i>Phytolacca dodecandra l'herit</i> leaves extract. ...	27
Figure 16. The chemical reaction for the synthesis of NiO NPs in the presence of plant extract.	30
Figure 17. UV-Vis spectra of NiO NPs and Cu-NiO NCs .....	31
Figure 18. The calculated band gap of the synthesized samples .....	32
Figure 19. The FT-IR spectrum of pure <i>Phytolacca dodecandra l'herit</i> leaves extract.....	32
Figure 20. The FT-IR spectrum of the synthesized NiO NPs and Cu-NiO NCs.....	33
Figure 21. X-ray pattern of NiO NPs and Cu-NiO NCs.....	36
Figure 22. SEM images of NiO (a), Cu-NiO (b), and their size distributions.....	38
Figure 23. Effect of pH on MB removal with catalyst. ....	39
Figure 24.Effect of initial dye concentration on photocatalytic degradation.....	40

Figure 25. Comparison of degradation of MB by sunlight with and without catalysts. ....	41
Figure 26. Effect of irradiation time and catalyst dose on Photocatalytic degradation .....	42
Figure 27. Recycling performance of particles. ....	43
Figure 28. Antioxidant activities of biogenically synthesized NPs and AA. ....	44
Figure 29. Predicted mechanism of H <sub>2</sub> O <sub>2</sub> scavenging activity. ....	44
Figure 30. UV-Vis absorbance of plant extract. ....	54
Figure 31. PZC OF Cu-NiO. ....	54
Figure 32. Methylene blue before and after photocatalytically degraded. ....	54
Figure 33. Optimization of different parameters of synthesizes. ....	56

## LIST OF TABLES

<b>Tables</b>	<b>pages</b>
Table 1. Comparison of Photocatalytic activity of NiO NPs with different photo catalysts. ....	7
Table 2. Phytochemical screening of the plant extracts.....	28
Table 3. FT-IR spectral peak values and functional groups of the plant extracts, NiO NPs and Cu-NiO NCs.....	34

## LIST OF ABBREVIATIONS AND ACRONYMS

P.d	<i>Phytolacca dodecandra l'herit</i>
NiO	Nickel oxide
Cu-NiO	Copper doped Nickel oxide
NPs	Nanoparticles
MB	Methylene blue
UV-Vis	Ultraviolet-Visible spectroscopy
XRD	X-ray diffraction
FT-IR	Fourier transformation infrared spectroscopy
eV	electron volt
ppm	Parts per million
PZC	Point of zero charge
SEM	Scanning Electron Microscopy
SPR	Surface Plasmon resonance
RNS	Reactive Nitrogen Species
ROS	Reactive Oxygen Species
NCs	Nanocomposites
VB	Valance Band
CB	Conduction Band
IC <sub>50</sub>	Half-maximal inhibitory concentration
pHPZC	pH at Point of zero charge.

## **ACKNOWLEDGMENT**

First and foremost I offer my thanks to Almighty God who helped me throughout my life. Next, I would like to thank my advisors Dr. Guta Gonfa and Mr. Ahmad Awol for their scientific guidance, support, and motivating me during the work of this research.

I also thank the chemistry department and staff members of the department, my classmates, and friends who shared with me their experiences, valuable information, and materials during the work of this research. I also thank Jimma university's material science engineering department for their support in FT-IR and XRD characterizations and Adama University for SEM readings.

My genuine acknowledgment is also extended to Ambo University, Ambo; Ethiopia, for sponsorship that they have given me to pursue my M. Sc. study.

Finally, I want to show my appreciation to all my family members for their continuous support in every way possible.

## ABSTRACT

Nanotechnology research is emerging as cutting-edge technology and nanoparticles and nanocomposites have played a significant role in the bioremediation and treatment of polluted water by organic and non-organic materials. Nanoparticles produced by plant extracts are more stable and biocompatible in comparison with those produced by physical and chemical methods. This research focuses on the synthesis of NiO NPs and Cu-NiO NCs using *Phytolacca dodecandra l'herit* (P. d) leaves extract and evaluation of their anti-oxidant and Photocatalytic activities. Cu-NiO NCs were synthesized using 50 mL of 0.1M Nickel (II) nitrate hexahydrate, 10 mL of 0.1M Copper (II) nitrate trihydrate and 20 mL of leaves extract. The synthesized nanoparticles were characterized by UV-Vis, XRD, FT-IR, and SEM, to study the energy band gap, average crystallite size, Functional groups, and morphology of the samples respectively. The UV-Vis analysis showed a red shift as copper doped indicating a decrease in the optical bandgap values. FT-IR characterization confirms the presence of various functional bands present in samples. Crystalline sizes of the formed particles were obtained to be 14.18 and 16.10 nm from the XRD data. SEM showed the crystallinity of particles with cubic structure. The Photocatalytic degradation of Methylene blue (MB) was found to be 78.3 and 97.8% by NiO NPs and Cu-NiO NCs respectively. In the antioxidant test, NiO NPs and Cu-NiO NCs prevented the oxidation of 50% of the H<sub>2</sub>O<sub>2</sub> molecules at a concentration of 363.96 µg/mL and 350.29 µg/mL respectively. Finally, the synthesized samples showed good photocatalytic and anti-oxidant activities.

**Keywords:** *Phytolacca dodecandra l'herit*, anti-oxidant, Photocatalytic, Nickel Oxide nanoparticles, Copper doped Nickel Oxide nanocomposites.

## Graphics Abstract.

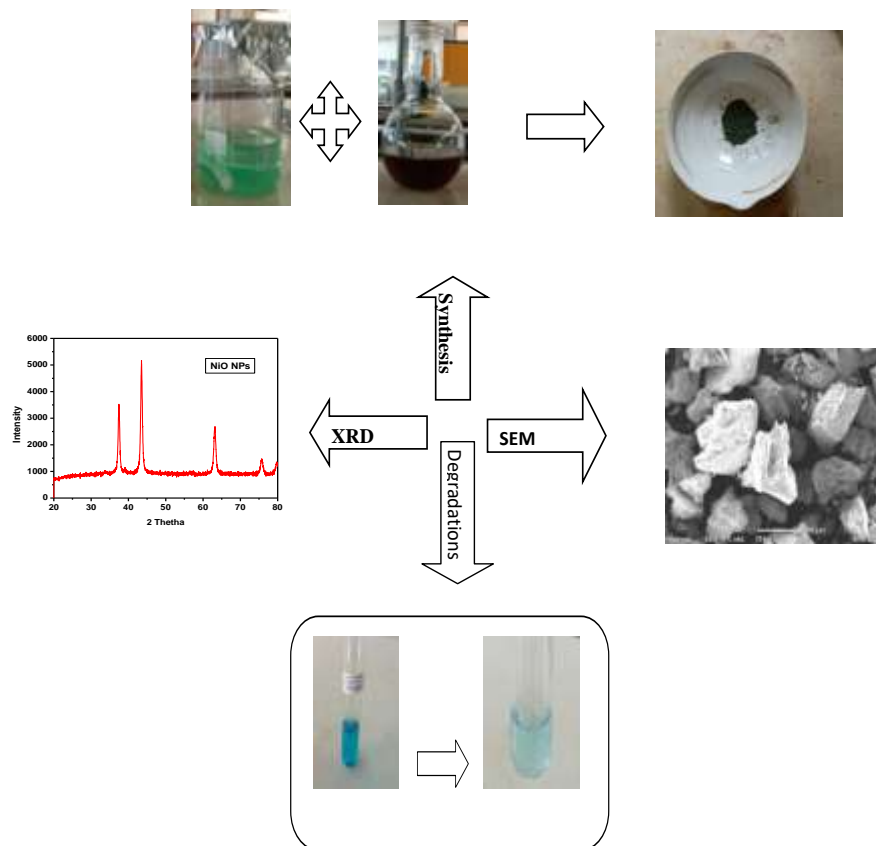


Figure 1. Graphics Abstract of the synthesized NPs using *Phytolacca dodecandra l'herit* leave.

# 1. INTRODUCTION

## 1.1 Background of the study

Water pollution is a global challenge that has increased in both developed and developing countries. It affects economic growth as well as the socio-environmental sustainability and health of billions of people. It is elevated in international and national priorities [1]. The dye is one of the most important classes of pollutants that result in colored wastewater that is sometimes hard to degrade because of its complex structure. Dye-containing wastewater generates from the textile, tannery, dying, pulp and paper, and paint industries. The majority of dyes arise from dyeing and finishing processes in textile industries. Dye pollutants result in several health hazards such as skin and eye-related diseases. Most dyes are toxic and pose a threat to aquatic living organisms [2].

To comply with strict environmental regulations, several conventional methods such as adsorption, membrane processes, biological processes, and electro coagulation have been utilized for the removal of dyes from water and wastewater. Conventional oxidation processes are not oxidizing dyestuff with complex structures, and thus advanced oxidation processes are introduced for dye degradation [3]. There are many methods for degradation of dyes in wastewater including physical, chemical, and biological approaches, but degradation and maintenance costs of most of these methods are high and some of these ways will produce a secondary waste product that needs further treatment, so using them for the treatment of wastewaters is not suitable and economical [2].

Antioxidants are molecules that can safely interact with free radicals, terminate the chain reaction, and convert them to a harmless molecule by donating an electron. In the recent decade, antioxidants have haggard attention due to their potential to minimize oxidative stress, which is defined as the pathophysiological response created due to the imbalance between the production of oxidants and the endogenous antioxidants to work against it. Hence, there is a net increase of the reactive oxygen species (ROS) including superoxide anions, hydroxyl radicals ( $\text{HO}\bullet$ ), hydrogen peroxide ( $\text{H}_2\text{O}_2$ ), singlet oxygen ( $^1\text{O}_2$ ), and reactive nitrogen species (RNS) (e.g., peroxyxynitrite, peroxy radicals). Free radicals with various chemical origins are very unstable, by extracting electrons from other molecules to reach equilibrium led to the degradation of the



target molecule. By scavenging free radicals, the harmful effects of free radicals such as cancer, heart disease, and neurodegenerative disorders may be minimized. As a result, there is a pressing need to devise some practical means of dealing with the world's serious problems [4]. Inorganic nanoparticles are thermally stable and chemically inert, which facilitate exploiting the potential, as well as the immobilization of natural antioxidants. Moreover, nanoparticles conjugated natural antioxidants facilitate chemical stability of the antioxidants in physiological conditions, convey the product in intact molecular form in a wider concentration range, and most importantly tender slow and continuous release [5].

Among metal oxide NPs, NiO NPs are capable to scavenge the ROS with high capability. NiO NPs synthesized by facile green combustion method using *limonia acidissima* natural fruit juice shows a significant hydroxyl radical scavenging activity [6]. Biosynthesized NiO NPs using *Raphanus sativus* (*R. sativus*) extract and calcined at 100 °C had the best antioxidant potential with an IC<sub>50</sub> of 258 gmL<sup>-1</sup> [7].

Nanoparticles have played a significant role in the bioremediation and treatment of polluted water by organic and nonorganic materials [2]. There are three fundamental practices for nanoparticles synthesis such as chemical, biological, and chemical approaches. Chemical and physical methods require more investment and consume more time which likely results in the toxic final product. Henceforth, the non-poisonous and least expensive natural (biological) methodology was picked for nanoparticles synthesis. Compared to other methods, the biological approach is eco-friendly. Most of the time the source for this approach was plant parts. The nanoparticles produced by plant extracts are more stable and biocompatible in comparison with those produced by physical and chemical methods [8]. In recent research, NiO NPs have drawn a greater interest, because of their unique properties, such as large surface-area-to-volume ratios, low porosity, high dispersion rates, high photo-absorption, and small heat capacities. Since particle size, morphology and high crystallinity influence the physicochemical properties; it is of great importance to synthesize NiO NPs with small particle size, which could enhance the efficiency of their applications. These unique properties of NiO NPs make viable and cost-effective surfaces suitable for different applications such as adsorbents, solar, fuel cells, catalytic agents, gas sensors, antibacterial materials and hydrogen storage [4, 5].

In the biological method, green synthesis plays a noteworthy job. There are several reports for NiO nanoparticles from green synthesis, towards their biological applications by using plant extract nanoparticles since using chemical methods have to disadvantage due to its toxicity and less eco-friendly, then synthesizing metal-doped metal oxide nanoparticles by biosynthesis method have varies advantages than Chemical one. Recently, NiO NPs have been synthesized using microorganisms, enzymes, and plant extracts. Ag<sub>2</sub>O and Co<sub>3</sub>O<sub>4</sub> NPs were prepared by using *Phytolacca dodecandra l'herit* leaf extracts [9, 10]. Biosynthesized NiO nanoparticles with different particle sizes for different applications including antioxidant activity by using extracts from plants such as *Sageretia thea (Osbeck.)* and *Stevia Leaf* extract [11, 12], has been reported and the results found are quite conclusive. However, we found as there is no report on the synthesis of NiO NPs and copper-doped NiO NCs by using *Phytolacca dodecandra l'herit* leaf extract.

In this work. The facile synthesis of NiO NPs and Cu-NiO NCs is reported using leaves extract of *Phytolacca dodecandra l'herit* as a reducing and stabilizing agent. The effects of various reaction parameters affecting the synthesis of NPs were also studied. The physicochemical characteristics were investigated through XRD, SEM, UV-Vis, and FTIR spectroscopy. Moreover, the photocatalytic and antioxidant activities of synthesized samples were investigated.

## **1.2 Statement of the problems**

*Phytolacca dodecandra l'herit* is used as traditional soap in rural area of Ethiopia. It is also used as traditional medicine against dandruff and other skin diseases. *P. d* produces a series of triterpenoid saponins that possess very potent and useful biological properties including antifungal, anti-protozoan, spermicidal, and insecticidal properties. The bioactivities of these plants can be enhanced more when it is supported with metal/metal oxide NPs, Surface reaction phenomenon of these biosynthesized particles (due to adsorbed antioxidant moiety onto the surface) and high surface area to volume ratio of particles generate a tendency to interact and scavenge the free radicals. On the other hand, metal/metal oxide nanoparticles play a great role in the removal of toxic pollutants to remediate a safe environment; however, the physical and chemical methods of synthesis of metal oxide NPs are expensive and not eco-friendly. Therefore, bio-synthesized metal oxide NPs based on green chemistry perspectives impose limited hazards to the environment and are relatively biocompatible methods for the production of NPs in an

eco-friendly manner. Thus, NiO-NPs and Cu-doped NiO NCs were synthesized using p. d leaf extract. The synthesized particles have the efficiency to remove toxic dyes to save environmental and health problems. Having the above pieces of evidence, the present study was intended to explore the photocatalytic activity of P. d leaf extract supported Cu-doped NiO NCs and evaluation of their antioxidant activities. Additionally, there were no reports for the synthesis of NiO NPs and Cu-doped NiO NCs by using P. d plant extract.

Based on this, in this study, the following questions were answered:-

1. Do phytochemicals from P.d plant extract act as a good stabilizing and capping agent for the copper-doped NiO NCs and NiO NPs formation?
2. Do the synthesized copper-doped NiO NCs and NiO NPs have potential in photocatalytic degradation and anti-oxidant capacity?
3. Is metal doping to metal oxide NPs enhance the dye degradation activity of the particles?

### **1.3 Objectives of the study**

#### **1.3.1 General objective**

The main objective of this study is to synthesize NiO NPs and Cu-NiO NCs using *phytolacca dodecandra l'herit* leaf extract and evaluate their anti-oxidant and photo-catalytic activities.

#### **1.3.2 Specific objectives**

- ❖ To prepare the P. d leaf extract
- ❖ To synthesize NiO NPs and Cu doped NiO NCs using the P. d leaf extracts.
- ❖ To characterize the synthesized samples using XRD, UV-Vis, FT-IR, and SEM.
- ❖ To study the photo-catalytic effect of the synthesized NPs and NCs.
- ❖ To study the antioxidant activity of NiO NPs and Cu doped NiO NCs.

### **1.4 The Significance of the study**

Green synthesis of nanoparticles was proven better method of synthesis due to slower kinetics, better manipulation, and their stabilization. Synthesizing nanoparticles with desired size and composition are of great interest as they provide solutions to various health and environmental [12] challenges. Therefore, the synthesized Nickel oxide and copper doped nickel oxide nanocomposites using *phytolacca dodecandra l'herit* leaf extract may provide the following significance.

1. The synthesized nanoparticles may be potential input for developing a drug in the future.
2. Enhance the knowledge about NiO NPs and Cu-doped NiO NCs.
3. The newly synthesized samples would serve as the baseline for the next research development by other researchers.
4. The newly synthesized samples may help in reducing environmental pollutions.

## 2. LITERATURE REVIEW

### 2.1 Nanoparticles

NPs, particles 1-100 nm in at least one dimension (1-D), have attracted great attention due to their extraordinary and fascinating properties and numerous applications over their bulk counterparts [13]. Among the various types of nanomaterials, nanostructured transition metal oxides deserve special consideration for their outstanding properties and technological applications [14]. Nanoscience and nanotechnology thus encompass a range of techniques rather than a single discipline and stretch across the whole spectrum of science, touching medicine, physics, engineering, and chemistry [15]. These materials are synthesized and characterized by various methods [16]. Nanoparticles can be classified based on their origin, Size, and Chemical composition [17].

#### **Metal oxide Nanoparticles**

Nanostructured metal oxides have been extensively discovered for various fundamental scientific and technological interests and to access new classes of functional materials with unique properties and noteworthy applications. In recent years, there has been an increasing interest in the synthesis of nanosized crystalline metal oxides because of their large surface areas, unusual adsorptive properties, surface defects, and fast diffusivities, conductivity, ionic structure, freezing, melting, and color, within the nano range [18].

#### **Nickel Oxide Nanoparticles**

In recent research, NiO NPs have drawn a greater interest, because of their unique properties. It belongs to a wide band gap (3.6 – 4.0 eV) p-type semiconductor. NiO with a cubic structure is well known because of its chemical stability and electrical properties [19]. The unique properties of NiO NPs make viable and cost-effective surfaces suitable for different applications such as adsorbents, solar and fuel cells, catalytic agents, gas sensors, magnetic and antibacterial materials. hydrogen storage, Photocatalytic degradation of organic dyes, pollutants from wastewater, and antimicrobial activity [8, 14, 18, 20–23]. It is also used as ant ferromagnetic layers, in lightweight structural components in the aerospace, inactive optical filters, cathode materials for alkaline batteries, and materials for gas or temperature sensors, such as Carbon monoxide sensors, Hydrogen sensors, and formaldehyde sensors [24]. As Adinaveen et al

[25]Propose a comparison of different photo-catalysts, the degradation activity of NiO NPs under UV light is highest as shown in table 1 below.

Table 1. Comparison of Photocatalytic activity of NiO NPs with different photo catalysts.

Materials Used	Biological Entity	Pollutant	Degradation efficiency (%)	Degradation time (min)
NiO	<i>Nepheliumlappaceum L</i>	Rhodamine B	92.3	180
ZnO	<i>Nepheliumlappaceum L</i>	Tannery wastewater	83.99	120
TiO <sub>2</sub>	<i>Jatrophacurcas L</i>	Methylene Orange	82.26	300
ZnO	<i>Pyruspyrifolia</i>	Methylene blue	80.3	210
ZrO <sub>2</sub>	<i>Ficusbenghalensis</i>	Methylene Orange	69	240

### NiO Nanocomposites

Different physical and chemical methods have been established to synthesize the NiO and transition metal doped NiO nanoparticles. When a narrow band gap semiconductor metal oxide nanomaterials are mixed with a broadband gap semiconductor material, the composite exhibits enhanced physicochemical properties compared with every single material. Nanocomposites have enhanced chemical, physical, and mechanical properties, which allow their application in industries as catalysts as well as for magnetic recording, biological uses, and nanomedicine. NiO doped with copper (Cu) has antibacterial and magnetic properties which are acceptable for biomedicines and spintronic applications. The nanostructures of copper oxide (CuO), as a p-type semiconductor material with a narrow band gap (1.2–1.4 eV), have been used broadly as catalysts, solar cells [19], visible-light-driven photo catalysts, and ultraviolet visible-light-driven photo catalysts and biosensors lithium-ion batteries [26].

### Strategies for Nanoparticles Synthesis

Principally there are two approaches used to synthesize NPs including the top-down approach and the bottom-up approach (figure 2).

**i) Top-Down Approach for NPs Synthesis.** This method comprises a set of synthetic technologies which synthesize NPs by removing certain parts from a bulk material substrate. The different methods for the removal of parts from bulk materials may include chemical,

electrochemical, and mechanical methods. The choice of a particular method is based on the material of the bulk substrate and the most wanted sizes of NPs. This technique however does not provide full control on particle size. The top-down method is extended to obtain nanosized area and coupled the mechanical removing systems with electrochemical and chemical techniques [27].

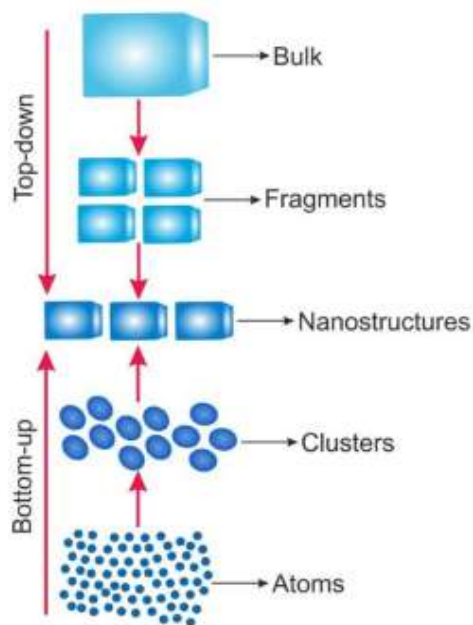


Figure 2. The schematic representation of the top-down and bottom-up approaches for the production of metal oxide nanostructures [28].

ii) **Bottom-Up Approach for NPs Synthesis.** This approach consists of a set of synthetic technologies which synthesize larger and more complex systems by stacking materials on the top of a base substrate and maintaining good control over the molecular structure. One of the basic requirements for this production approach is that there must be strong adhesion forces between the surface layer and base substrate and for this purpose surfactants are added which increases the adhesion among the surface layer and base substrate [27].

NPS can be prepared by physical, chemical, or biological methods (figure 3) [29].

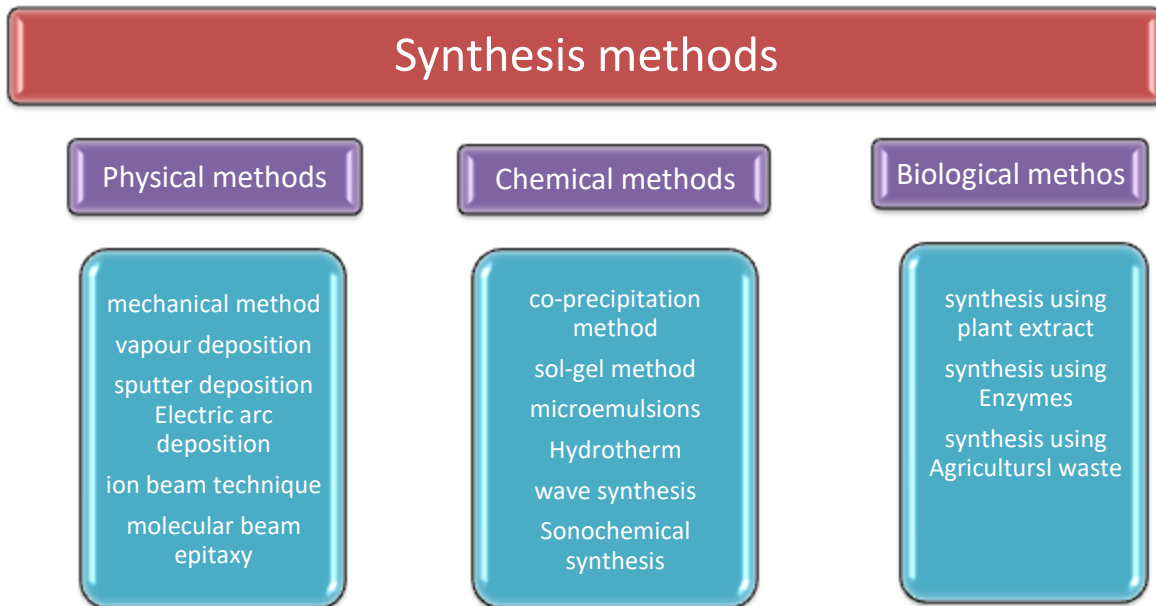


Figure 3. Different methods for synthesizing nanoparticles [30]

There is a big concern to search for environmentally-helpful methods which result in the development of bionanotechnology. Bionanotechnology synthesizes NPs by using biological systems including bacteria, fungi, yeast, plants, and naturally occurring small molecules such as vitamins, proteins, peptides, and reducing sugars. Biological synthesis provides an environmentally friendly, simple, inexpensive approach for synthesizing NPs with an added advantage of stabilizing the formed NPs as plant secondary metabolites besides acting as synthetic agents also acting as a capping agent [27].

## 2.2 Green synthesis

Green protocols for the synthesis of nanoparticles have been attracting a lot of attention because they are eco-friendly, rapid, and cost-effective. likewise, NPs synthesized by using green chemistry have no or little cytotoxicity as compared to chemically synthesized NPs [27, 31]. For a long time, plants have shown the capability to absorb hyper accumulate and decrease inorganic metallic ions from the surrounding environment. It is now well established that various organic components present in plant tissues are capable of acting as effective biological factories to significantly reduce eco-friendly contamination, and can recover metals from industrialized waste. Moreover, mixtures of molecules identified in plant extracts can act as both stabilizing



(capping) and reducing agents all through NPs synthesis[31, 32]. Some of the vital plant phytochemicals are shown in Figure 4.

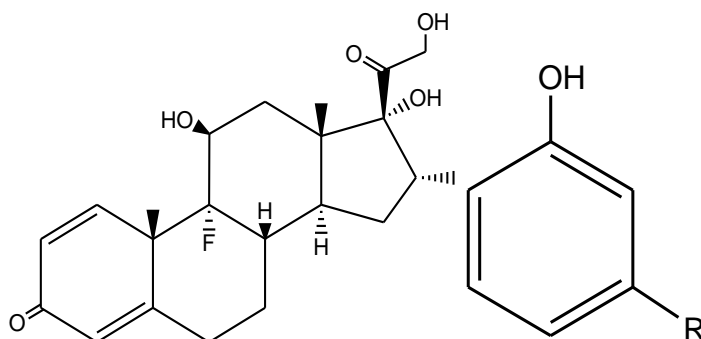


Figure 4. Chemical structure of Steroid (dexamethasone) (A) and phenolic acid (B)[33].

### 2.2.1 Mechanism of Green Synthesis

The secondary metabolites of plants are answerable for the reduction of metal ions into metal atoms. The metal salts like nitrates, chlorides, oxides, and sulfates have high reduction potential due to the attachment of metal with the chloride, oxide, and sulfide parts and their tendency to donate electrons. As a result of both these issues electronic density on the conjugative salts of metal increases. So metals in their ionic form can easily get detached from their anionic part and get reduced into stable form by using plant extract. The secondary metabolites of plants, including alkaloids, flavonoids, polyphenols, and terpenoids act as a chelator to metal ions and reduce them into zero-valent states. Mostly the  $\text{OH}$  group of polyphenols and flavonoids develop coordination with metal ions. We can describe the mechanism of plant-mediated synthesis of metal and metal oxide NPs by considering the following three phases: activation phase involves the reduction of metal ions and reduced metal atoms undergo nucleation; growth phase involves the spontaneous coalescence of small adjacent NPs into larger size NPs, that is, Ostwald ripening (a process in which NPs are directly formed through heterogeneous nucleation and growth and further reduction of metal ion); this process enhances the thermodynamic stability of NPs; Termination phase decides the final shape of NPs. In the case of metal oxide NPs, the end product is air dried or calcined in air to get the final metal oxide NPs [29] as shown in figure 5 below.

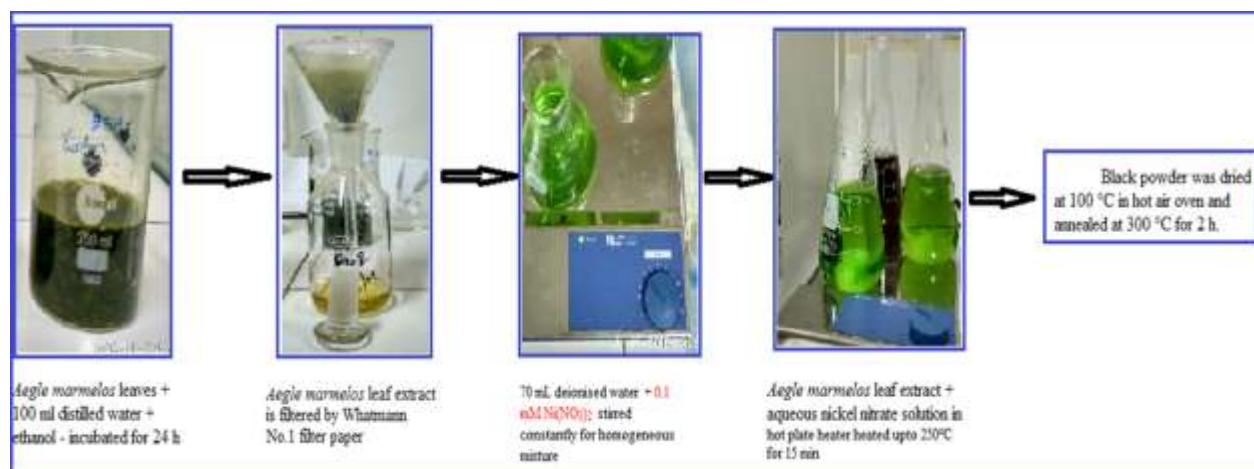


Figure 5. Graphics Abstract of Preparation of nickel oxide nanoparticles using *Aegle marmelos* leaves [34].

The nature and concentration of the plant extract, pH, temperature, metal salt concentration, and contact time are known factors affecting the green synthesis of NPs [29].

### 2.2.2 *Phytolacca dodecandra l'herit*

*Phytolacca dodecandra l'herit* is native to sub-Saharan Africa and Madagascar. It is a member of the Phytolaccaceae family, and is commonly known in Ethiopia as “endod.” Other local names include soapberry, African soapberry (English). The plant is a sprawling woody climber with an average length of stems that reaches 5 to 8 m. It grows rapidly especially during the rainy season with erect, racemic, dioecious flowering stalks, and red berries (figure 6). *P. d* has different medicinal and nonmedicinal uses. The dried powdered berries of *P. d*, when sited in water, form a foaming detergent solution. Therefore, Ethiopia, Somalia, and Uganda have traditionally been using the detergent solution for cleaning clothes for a century. In East, central Africa, and Madagascar, extracts of berries, seeds, leaves, and roots have also been used traditionally as a purgative, anthelmintic, laxative, emetic, diuretic, and ant diarrheal for humans and purgative for animals. The leaves juice and crushed roots and berries were applied to wounds for skin diseases such as ringworms, scabies, leprosy, boils, and vitiligo. In Congo, an infusion of berries or roots is taken orally to treat rabies, malaria, sore throat, and respiratory problems. Boiled leaves are also used to treat asthma and tuberculosis. In Tanzania, macerated root bark or leaves are used for the treatment of epilepsy. In southern Nigeria, the leaf decoction is used as a laxative in a newborn baby. In Rwanda, leaf juice is used to treat otitis media, and the young leaves and shoots are chewed to induce abortion [9 -24].



Figure 6. *Phytolaccadodecandra l'herit* plant

### **The phytochemical constituent of *Phytolacca dodecandra l'herit* leaf.**

The results of the different preliminary phytochemical screening tests showed the presence of bioactive compounds in the extract of *P. d* leaves in a polar solvent such as water and methanol showed that the plant has various secondary metabolites like alkaloids, protein and amino acids, saponins, flavonoids, terpenoids, total phenols and tannins [25].

### **Phenolic compounds.**

Phenolic compounds are the major class of secondary metabolites in plants and are divided into phenolic acids and polyphenols. These compounds are found combined with mono- and polysaccharides, linked to other phenolic groups, or can occur as derivatives, such as ester or methyl esters. Among the several classes of phenolic compounds, phenolic acids, flavonoids, and tannins are regarded as the main dietary phenolic compounds.

The hydrogen atoms of the adjacent hydroxyl groups (o-diphenol), placed in various positions of the rings A, B, and C, the double bonds of the benzene ring, and the double bond of the oxo functional group ( $-C=O$ ) of some flavonoids, provide these compounds their high antioxidant activity (figure 7). This characteristic can be observed in quercetin and catechin [35].



compounds containing 27 carbon atoms forming the core structures: spirostan ( $16\beta,22:22\alpha$ ,26-diepoxy-cholestan) and furostan ( $16\beta,22$ -epoxycholestan) [37].

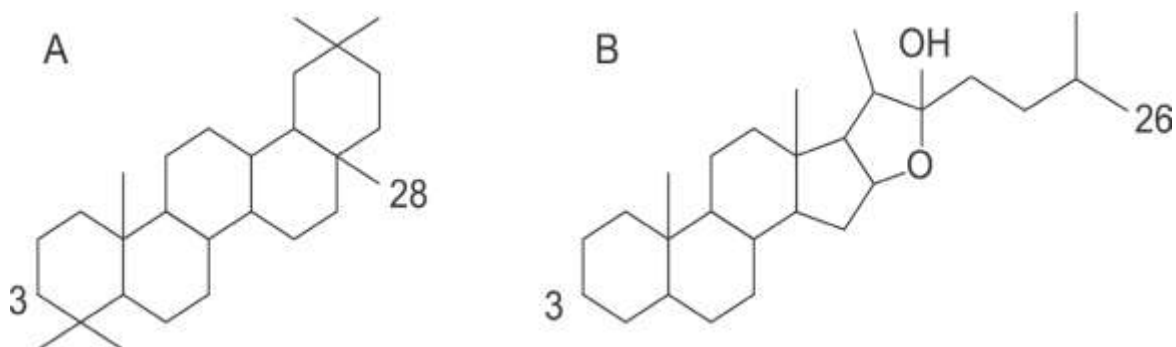


Figure9. Structures of (A) triterpenoid and (B) steroidal saponins

### Flavonols

Flavonoids are a huge group of natural substances with changeable structures present almost in all growing parts of the plants, being reported as the most abundant plant pigment along with chlorophyll and carotenoids, also providing fragrance and taste to fruits, flowers, and seeds, which makes them attractants for other organisms. These compounds are also one of the largest groups of secondary metabolites (Figure 10). further their relevance in plants, flavonoids are essential for human health because of their high pharmacological activities [38].

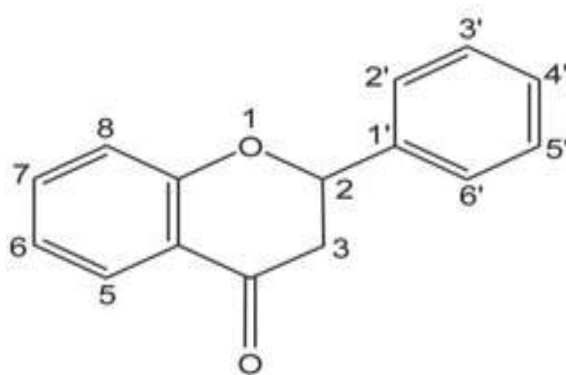


Figure 10. Flavonoids subgroup structure.

## **2.3 Characterization technique for metal and metal oxide nanoparticles**

### **2.3.1 UV-Vis spectroscopy**

UV-Vis spectroscopy uses light in the visible ranges or its adjacent ranges. The color of the chemicals involved directly affects the absorption in the visible ranges. Molecules undergo electronic transitions in these ranges of the electromagnetic spectrum [39]. The Principle of UV-Vis Spectroscopy is based on the absorption of ultraviolet light or visible light by chemical compounds, which results in the production of distinct spectra. UV-Vis spectroscopy was used to show the band gap energy of synthesized nanoparticles. The band gap increases with decreasing particle size and the absorption edge are shifted to higher energy (blue shift) with decreasing particle size [40].

Electronic spectra are used to identify and determine the energy of d-d electronic transitions and electronic charge transfers. The plots of variation of  $(\alpha h\nu)^n$  versus  $h\nu$  for the NiO and Cu-NiO NPs were presented. These plots are known as Tauc's plots and they are used to find out the accurate optical band gap value by the extrapolation of the linear part. This suggested that the optical transition in the sample is indirect or direct [15] and it is used to calculate an optical band gap of the nanoparticles. Tauc plot has the photon energy ( $h\nu$ ) on the X-axis and a quantity  $(\alpha h\nu)^2$  on the Y-axis and extrapolating the linear portion of the curve to the X-axis yields the band gap energy of the material [41].

### **2.3.2 Fourier Transformation Infrared (FT-IR) Spectroscopy**

Infrared spectroscopy is an essential device to characterize the structure of matter at the molecular scale. FT-IR spectroscopy analysis is a method based on the principle of infrared spectroscopy, and it has extended its area of application to the study of nano-scaled objects during the last decade [42].

FT-IR Spectroscopy has a large application range, from the analysis of small molecules or a molecular complex to the analysis of complexes [17]. Infrared spectroscopy probes the molecular vibrations. Functional groups can be associated with characteristic infrared absorption bands, which correspond to the fundamental vibrations of the functional groups [43]. FT-IR spectrometer involves an examination of the twisting, bending, rotation, and vibrational modes of the atoms in a molecule upon interaction with infrared radiation portion of incident radiation

are observed at a specific wavelength and functional groups of the sample can be identified from the spectrum [15].

FT-IR is very useful to study surface chemistry and identify the possible biomolecules for the capping and stabilization of nanoparticles [29]. The possible functional groups that are present in the plant extract and synthesized nanoparticles are identified in the ranges of 4000-400  $\text{cm}^{-1}$ [44].

### **2.3.3 X-ray diffraction (XRD)**

Powder XRD was used to determine the identification of purity and quantitative analysis of nanoparticles is explained by the XRD pattern [15]. For phase identification, XRD patterns are collected on an X-ray diffractometer. These X-rays are generated by a cathode ray tube, filtered to produce monochromatic radiation, collimated to concentrate, and directed toward the sample [45]. The atomic planes of a crystal cause an incident beam of X-rays to interfere with one another as they leave the crystal. XRD is a non-destructive technique used to identify crystalline phases and orientation, measure the thickness of thin films and multi-layers, determine atomic arrangement [8] and structure of the NPs [29]. XRD technique is also used to get information like lattice parameters, the crystallite size of crystals, defects, and strains [45].

The average crystallite size of the nanoparticles was calculated using Scherrer's formula [46].

$$D = \frac{k\lambda}{\beta \cos \theta} \dots \dots \dots (1)$$

Where D is grain size, K is an empirical constant to 0.9 and  $\lambda$  is the wavelength of the incidence beam ( $\lambda=1.5406\text{\AA}$ ) [4].  $\beta$  is the full-width half maximum (FWHM)in radian, and  $\theta$  is the angular of the peak position.

### **2.3.4 Scanning electron microscopy (SEM)**

The scanning electron microscope is a very useful instrument to get information about topography, morphology, and composition information of materials. It is a type of electron microscope capable of producing high-resolution images of a sample surface. SEM images have a characteristic three-dimensional form and are useful for judging the surface morphology of the sample [47]. This technique provides information regarding the species present at different depths of the sample. SEM may be used to determine the crystallography of (poly) crystalline samples and individual crystallite orientations, as well as crystallographic parameters

of the sample. Sample simply deposited onto the top of an adhesive fastened to an aluminum stub/holder. Most often, conductive carbon tape is used to sequester the sample. Computer software was used to collect/analyze the resulting patterns to determine the crystallography of the material. The morphologies of the phytomolecules-coated NiO nanoparticles [48] and Cu-NiO nanostructures were studied using SEM [11].

The SEM instrument is based on the principle that the primary electrons released from the source provide energy to the atomic electrons of the specimen, which can then release as the secondary electrons (SEs) and an image can be formed by collecting these secondary electrons from each point of the specimen [49].

#### **2.4. Dyes**

Dyes are colored compounds that are widely used in textiles, printing, rubber, cosmetics, plastics, leather industries to color their products results in generating a large amount of colored wastewater. Among all the dyes used in industries, textile industries were placed in the first position in using dyes for the coloration of fiber. Dyes are chemical compounds that attach themselves to textile or surface shells to impart color. Depolarization of wastewater from textile and manufacturing industries is a major challenge for ecological managers as dyes are water-soluble and produce very intense colors in water with acidic properties [50].

#### **Sources of dyes**

Dyes are mainly derived from natural sources without any chemical treatment such as plants, insects, animals, and minerals. Dyes resulting from plant sources are indigo and saffron, insects are cochineal beetles and lac scale insects, animal sources are derived from some species of mollusks or shellfish, and minerals are ferrous sulfate, ochre. Industries such as textile, printing, paper, carpet, plastic, and leather use dyes to provide color to their products. These dyes are always left in industrial waste and consequently discharged into the water body. Dyes are released with wastewater from various industrial outlets. The textile manufacturing and dyeing industries utilize more quantities of a large number of dyes and release these dye pollutants into the environment as wastewater effluents. These dyes are highly toxic and even carcinogenic to microbial populations and mammalian animals hence these are needed to remove from the water effluents before they are released into water bodies. Dyes are stable to light and not biologically



degradable; they are resistant to aerobic digestion and signify one of the hard groups to be removed from the industrial wastewater [50].

### Dye removal techniques

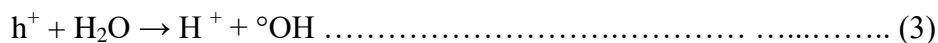
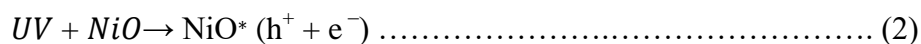
Dyes are extensively used in the textile, plastic, leather, cosmetic, paper, food, and pharmaceutical industries to color the final products. Industrial wastewater containing even small amounts of dyes can severely affect the environment and cause problems to human health and aquatic life as shown in figure 11 below [15].

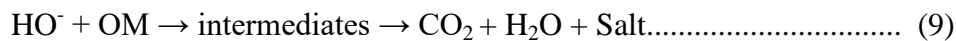
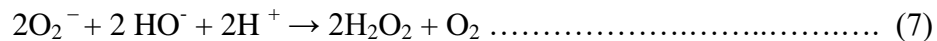
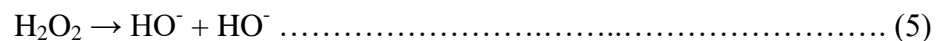
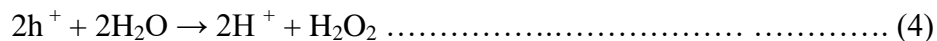


Figure 11. The Pollutant and affected water body by organic dyes

There are many conventional methods available to remove dyes from industrial wastewater (effluents). These include biological treatment, electro dialysis, ozonation, coagulation/flocculation, adsorption on a solid phase, membrane separation, electrochemical oxidation, ultra-filtration, sorption-floatation, and Fenton/Photo-Fenton oxidation. However, these methods have several limitations like; Biological treatment methods involve a long reaction time and emit bad odors, Incineration can produce toxic volatiles gases, Ozonation presents a short half-life (20 min), while the stability of ozone is strongly affected by the presence of pH, salts, and temperature, Expensive, ineffective, and result in high levels of sludge and by-products [15].

The photocatalysis process can degrade toxic organic pollutants into less toxic by-products through mineralization, ensuring zero waste production. The different mechanisms for the Photocatalytic activities of pure NiO NPs have been proposed as the following [51, 52].





The several steps containing possible mechanisms for sunlight-mediated degradation of Organic dye was shown in Figure 12 and 13.

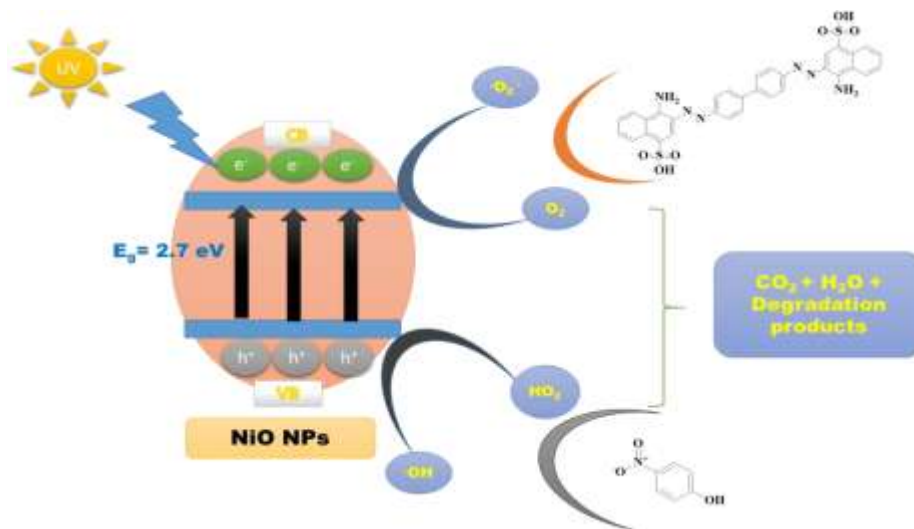


Figure 12. Photocatalytic degradation mechanism of CR over NPs [2].

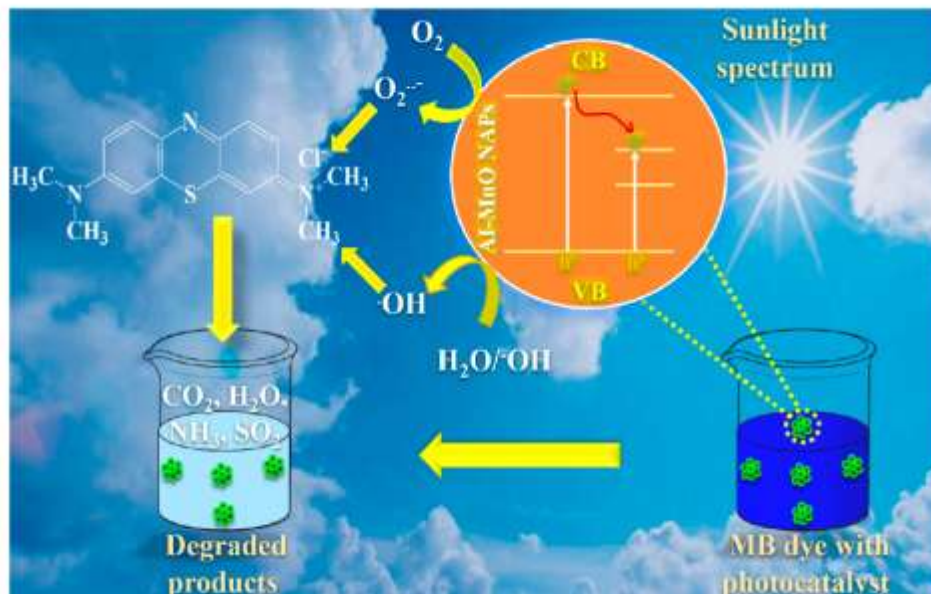


Figure 13. Photocatalytic degradation mechanism of Methylene blue (MB) dye by the green-synthesized Al-MnO NPs using leaf extract of *Abutilon indicum* [53] under visible light.

Photocatalytic degradation by NPs in wastewater treatment has numerous advantages over the physical, chemical, and biological methods available to date. These include; Rapid oxidation, No formation of polycyclic products, and oxidation of pollutants (up to the ppb level), Chemical stability, Optical and electrical properties, Effective, inexpensive, and eco-friendly method [29]. Conventional treatment methods are capable of color removal from wastewater but are incapable of complete mineralization. UV-light-driven photo-catalysis is an emerging technique for the mineralization of dye-containing wastewater. Normal bandgap excitation and photo-oxidation process occur under UV light. In the presence of visible light, dye degradation is also possible via a dye-sensitization pathway in the presence of a sensitizing dye [54].

Recently, Arun et al [19] had investigated the biogenic synthesis of nanostructured CuO and CuO/NiO nanocomposites using *Azardicaindica* leaf extract as a reducing agent and identify its degradations by two dangerous water pollutants comprising MB and eosin yellow. But they do not use cost-effective methods. Thus, this study is going to solve this problem by using only sunlight and catalysts to degrade the pollutants.

## 2.5. Antioxidant.

Antioxidants are compounds capable of inhibiting the oxidation of other molecules. Antioxidants are able to either delay and inhibit the oxidation processes which take place under the influence of atmospheric oxygen or reactive oxygen species. The body does not have too much antioxidative defense system, so if there is exposure to extreme free radicals, the body needs exogenous antioxidants. Studies show that phenolic compounds such as flavonoids have an antioxidant activity of free radical catchers found in plants, fruit, and leaves which are commonly used as traditional medicine [55].

Among reactive oxygen species (ROS), hydrogen peroxide ( $\text{H}_2\text{O}_2$ ) is a relatively stable, non-radical oxidant.  $\text{H}_2\text{O}_2$  causes toxicity via two main mechanisms: it leads to depletion of adenosine triphosphate (ATP), reduced glutathione (GSH), and reduced nicotinamide-adenine dinucleotide phosphate (NADPH), and produces strand breaks in DNA that trigger energy-consuming DNA repair mechanisms and activate the nuclear enzyme poly(adenosine diphosphate [ADP]-ribose) polymerase (PARP) activity leading to cell death by the so-called enzyme-suicide mechanism [56]. The reaction mechanism for the interaction between Au NPs and  $\text{H}_2\text{O}_2$ /superoxide is shown in figure 13 [57].

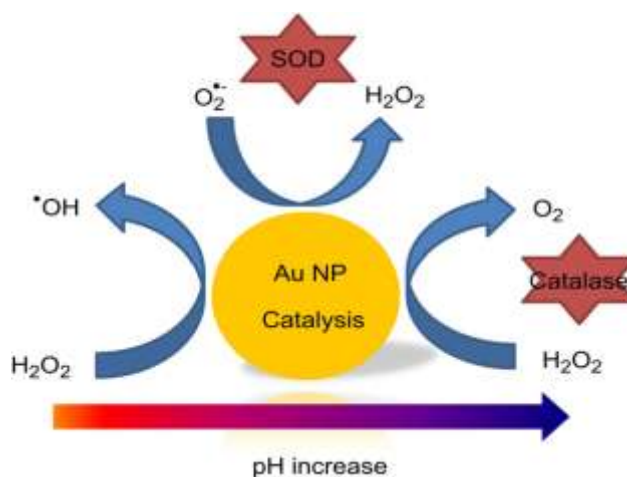


Figure 14. Scheme of Illustration of catalytic properties of Au NPs in decomposing  $\text{H}_2\text{O}_2$ .

Recently, Srihasam et al [11] had investigated the Phytogetic generation of NiO NPs Using *Stevia* Leaf Extract and Uddin et al[58] shows plant-mediated NiO NPs exhibited strong antioxidant activities.

Literature studies demonstrated that nanocomposites are more effective photocatalysts for the degradation of dyes; combinations of two individual metals may be more efficient than either individual. Among different methods, photocatalysis using NPs as an alternative to physical, chemical, and biological methods shows great potential. Generally, nanoparticles are synthesized by various routes including eco-friendly and inexpensive green synthetic methods [29], and physicochemical characteristics methods like XRD, SEM, UV-Vis, and FT-IR spectroscopy can be used to characterize the synthesized NPs.

### 3. MATERIALS AND METHODS

#### 3.1. The study area and period

The study was carried out from March to July 2021; at the Chemistry laboratory, Jimma university's main campus, and 346 km southwest of Addis Ababa, Ethiopia.

##### 3.1.1. Materials

*Phytolacca dodecandra l'herit* leaf was collected from Jimma university garden, Jimma, Southwest Ethiopia.

##### 3.1.2. Chemicals

Nickel nitrate hexahydrate, methylene blue, hydrogen peroxide, sodium hydroxide, phosphate buffer, sulfuric acid, nitric acid, chloroform, Wagner's solution, ferric chloride, concentrated hydrochloric acid, ascorbic acid, and distilled water was used.

##### 3.1.3. Apparatus and equipment

Oven, Mortar and Pestle, Digital balance, Hot Plate and Magnetic bar, Centrifuge, Filter paper, Beakers, Test tubes, Droppers, Graduated cylinders, Cuvettes, Erlenmeyer flask.

##### 3.1.4. Scientific instruments

The Crystalline nature and size were identified with the aid of the X-ray diffractometer. The FT-IR spectrometer was used to examine the functional groups. The morphology of the sample was studied by Scanning Electron Microscopy. Absorption spectra were recorded with the UV-Vis spectrophotometer [59].

#### 3.2. Sample collection and preparation

The *Phytolacca dodecandra l'herit* (P. d) leaves were collected by random sampling technique and thoroughly cleaned with tap water to remove debris and other contaminants, followed by distilled water and air-dried at room temperature. The dried sample was ground with mortar and pestle, then the aqueous extract of the leaf was prepared by boiling 10 g of the leaves with 100 mL of distilled water at about 60 °C for 20 min [19]. The extract was cooled to room temperature and filtered using Whatman No. 1 filter paper. Finally, the extract was stored to be used for further experiments [8].

### **3.3. Phytochemical test of *Phytolacca dodecandra* L'herit leaves extract.**

#### **3.3.1. Test for flavonoids**

**Alkaline reagent Test:** 1 mL of the extract was treated with 5 mL of NaOH. The presence of flavonoids was confirmed by the formation of the intense yellow color [60].

#### **3.3.2. Test for alkaloids**

**Wagners Test:** 1mL of the solvent extract was acidified with 1mL of 1.5% v/v of HCl and 1mL of Wagner's reagent was added. the occurrence of alkaloids was indicated by the formation of yellow and/or brown precipitates [61].

#### **3.3.3. Test for saponins**

**Frothing Test:** About 1 mL of the extract was diluted separately with 20 mL of distilled water and was shaken in a graduated cylinder for 15 min. A 1 cm layer of foam was formed which indicates the presence of saponins [60].

#### **3.3.4. Test for tannins and phenolic compounds**

**Ferric chloride test:** 1 mL of the extract was treated with a few mL of 5% neutral ferric chloride. The formation of a dark blue and/or bluish-black color product showed the presence of tannins and Phenol [60, 61].

### **3.4. Synthesis of nickel oxide nanoparticles**

The synthesis was taken place according to Ahmad et al [26] with some modifications. To synthesis NiO NPs 50 mL of 0.1M nickel (II) nitrate hexahydrate ( $\text{Ni}(\text{NO}_3)_2 \cdot 6\text{H}_2\text{O}$ ) was stirred for 20 min, then 20 mL of leaves extract was added drop wise. The mixture was progressively stirred for 30 min at room temperature. To adjust the pH of the solution 5 M NaOH was added drop by drop. The resulted product was stirred at room temperature for 2 hr. Subsequently, the obtained solid was filtered and washed several times with distilled water and ethanol to remove impurities. Nanoparticles were dried at 70 °C for 2 hr in the oven. Finally, it was ground with mortar and pestle to obtain the final nanoparticles.

### **3.5. Synthesis of copper doped nickel oxide nanocomposites**

To synthesis Cu-NiO NCs according to Ahmad et al [26] with some modification, 50 mL of 0.1M Nickel (II) nitrate hexahydrate ( $\text{Ni}(\text{NO}_3)_2 \cdot 6\text{H}_2\text{O}$ ) was stirred for 20 min, then 10 mL of 0.1M Copper (II) nitrate trihydrate was added drop wise followed by the addition of 20 mL of

leaves extract was added dropwise. The mixture was progressively stirred for 30 min at room temperature. To adjust the pH of the solution 5 M NaOH was added drop by drop. The resulted product was stirred at room temperature for 2 hr. Subsequently, the obtained solid was filtered and washed several times with distilled water and ethanol to remove the impurities. Nanocomposites were dried at 70 °C for 2 hr in the oven. Finally, it was ground with mortar and pestle to obtain the final nanocomposites.

### **3.6. Physicochemical Methods of Characterization**

#### **UV-Vis Analysis**

The electronic spectra of the NiO NPs and Cu-NiO NCs in solution were run in the range of 300-800 nm on a 6705 UV/Vis spectrophotometer (jenway). Generally, surface plasmon resonance of synthesized nanoparticles and energy band gap of synthesized samples were analyzed by UV-Vis spectroscopy.

#### **FT-IR Analysis**

Fourier Transform Infrared (FT-IR) spectra recorded in 4000-400  $\text{cm}^{-1}$  were used to identify the presence of functional groups and to receive valuable information regarding the presence of ligand in the metal NPs as KBr discs pest on a Perkin Elmer. FT-IR technique was used to obtain an infrared spectrum of absorption/emission of solid and gather spectral data in an extensive spectral range.

#### **XRD Analysis**

The crystallinity and crystalline phase of synthesized samples were determined through X-ray diffraction (XRD) profiles (DR AWELL XRD -700 using  $2\text{CuK}\alpha$  radiation) in  $2\theta$  range of  $20\theta$  to  $80\theta$  with a scan speed of  $0.03^\circ/\text{min}$ .

#### **SEM Analysis**

The morphological features of the prepared NiO NPs and Cu-NiO NCs nanostructures were studied using scanning electron microscopy (JCM-6000Plus). Sample simply deposited onto the top of an adhesive fastened to an aluminum stub/holder. Computer software was used to collect/analyze the resulting patterns to determine the crystallography of the material.



### 3.7. Photocatalytic degradation of dye

To evaluate the Photocatalytic performance of the as-prepared sample towards the degradation of MB dye, 20 mg of the prepared samples (NiO nanoparticles or Cu-NiO nanocomposites) were dispersed in 100 mL of 10 ppm MB dye solution using sunlight irradiation as a source of light. The suspension was stirred in dark for 30 min before exposing to sunlight to ensure adsorption/desorption equilibrium between photo catalysts and dye solution. Then, the system was illuminated under sunlight with continuous stirring. Aliquots of 5 mL were collected at regular intervals of time and centrifuged for 3 min. The UV-Vis absorbency of centrifuged samples was then carried out by UV-Vis spectrometer. The degradation of the blank was determined similarly. The percentage degradation was determined by using the following equation:

$$\% \text{degradation} = [(C_0 - C_t) / C_0] \times 100 \dots \dots \dots (10)$$

Where:  $C_0$  is the initial concentration of dye and  $C_t$  is a concentration of dye at any time  $t$  [62].

### Reusability performance of the nanoparticles/nanocomposites.

To study its recyclability, the optimized catalyst doses (0.06 gm) of NPs were allowed to settle by centrifugation after the Photocatalytic degradation for 120 min (10 mg/L). The recovered catalysts were then collected and reused 2 times under the same photo degradation conditions according to the literature [3].

### 3.8. Antioxidant Activity

The hydrogen peroxide scavenging activity was determined according to the method of Cetinkaya et al [63]. 0.1 mL of different concentrations of the synthesized particles and ascorbic acid (50-1000  $\mu\text{g} / \text{mL}$ ) were mixed with hydrogen peroxide (0.6 mL, 50 mM) prepared with phosphate buffer (pH 7.4). This reaction mixture was incubated for 10 min. The absorbance was measured spectrophotometrically at 230 nm using phosphate buffer as blank. The percent of hydrogen peroxide scavenging was calculated using equation 12.

$$\% \text{ scavenging activity } [\text{H}_2\text{O}_2] = [(A_0 - A_1) / A_0] \times 100 \dots \dots \dots (11)$$

Where:  $A_0$  = Absorbance of control,  $A_1$  = Absorbance of the sample [64, 65].

## 4. RESULTS AND DISCUSSIONS

### 4.1. Phytochemical analysis of *Phytolacca dodecandra l'herit* leaves extract

The phytochemical test was conducted for justification of different types of bioactive compounds that appear in the *Phytolacca dodecandra l'herit* leaves extract by using a different type of chemical and it is shown in figure 15. Correlation between the phytoconstituents and the bioactivity of a plant is desirable to know for the synthesis of compounds with specific activities.



Figure 15. Results of the Phytochemical test of *Phytolacca dodecandra l'herit* leaves extract.

The *Phytolacca dodecandra l'herit* plant leaves extract was made by a simple decoction method using distilled water. The red-colored extract was obtained. The most important bioactive constituents of the plants were summarized in table 2. This result has a close agreement with the literature [60, 61].

Table 2. Phytochemical screening of the plant extracts.

S/No	Phytochemical	chemical tests	results
1	Phenolic	ferric chloride	+
2	alkaloids	Wagner`s test	+
3	saponins	frothing test	+
4	tannins	ferric chloride	+
5	flavonoids	alkaline reagent	+

+ .... indicates the presence of phytochemicals

## 4.2. Synthesis.

### 4.2.1 Synthesis of NiO NPs

During the synthesis of NiO NPs, the color of the precursor was bright green, and leave extract was red, after reaction brown color was observed which indicates the formation of NiO NPs. During the synthesis of these NPs, Phytochemicals present in the plant extract act as the reducing agent to convert metal ions to their corresponding nanoparticles and simultaneously act as an effective capping agent to prevent the NPs agglomerations as revealed by literature [66].

### 4.2.2. Synthesis Cu-NiO NCs

During the synthesis of Cu-NiO NCs, a mixture of nickel nitrate hexahydrate and copper nitrate trihydrate was green at the beginning. After the leave extract was added, the deep green color was observed which indicates the formation of Cu-NiO NCs. During the synthesis of these NCs, Phytochemicals present in the plant extract act as the reducing agent to convert metal ions to their corresponding nanoparticles and simultaneously act as an effective capping agent to prevent the NCs agglomerations as stated by literature [66].

### 4.2.3. Optimization of different parameters.

#### 4.2.3.1. Concentrations of precursor

The ratio of the concentration of precursor must correspond to the volume of plant extract used [67]. In this study, 50 mL of different precursor's concentrations (0.05, 0.02, 0.03, 0.1, and 0.2) M were reacted with 20 mL leaf extracts and 0.1 M was optimized because it gave a sharp peak which shows the formation of nanoparticles since the intensity of the surface Plasmon peak has direct proportionality with the concentrations of synthesized nanoparticles in the solution [68]. The result obtained was in close agreement with a recent report [69] and an increase in intensity suggests that more nanoparticles are formed [70].

#### **4.2.3.2. Varying volumes of extract**

The synthesis of NPs using plants extract is mainly influenced by the types of bio-molecules found in plant extracts and the volume used. The volume of plant extracts used in the synthesis of nanoparticles plays a significant role in the reduction of metal ions to reduced metal in their oxidation number [71]. To identify the optimum volumes of plant extracts, different volumes (10, 20, 30, 40, and 50) mL were reacted at the fixed volume of precursors. In this manner, the 20 mL was optimized by giving the smallest wavelength. This is attributed that Phytochemicals present in the plant extract, which are responsible for the bio reduction and stabilization of the NPs [72] react with precursor.

#### **4.2.3.3. Varying reaction time**

Reaction time is essential to the synthesis and stability of nanoparticles [73]. The effect of reaction time was evaluated during the green synthesis of nanoparticles. Different reaction time 20 to 180 min by a difference of 10 min and 120 min was optimized. With this min intensity of UV-Vis peak increased which shows all precursors were reacted with leaves extract and reduction in metal ions was completed.

#### **4.2.3.4. Effect of pH**

The pH was one of the factors that influenced the size, shape, and composition of nanoparticles [74]. The effect of pH on the formation of NiO NPs has been evaluated by UV-Vis spectroscopic studies. pH in aqueous media can highly influence the progress of the metal ion reduction reaction [75]. The role of pH on NPs synthesis could be seen in its effect on the capping and stabilizing abilities, and consequently the growth of the nanoparticles. The presence of OH<sup>-</sup> ion

in an alkaline pH environment might enhance the reducing and stabilizing capabilities of the biomolecules in the leaf extract [76].

To know the optimum pH value of NPs, pH range from 5 to 11 were treated. At pH 10, a blue shift was observed that could be attributed to the decrease in the particle size. Therefore, pH 10 was optimized. Above pH 10, it was not able to synthesize NiO NPs, as may be the high OH ion concentration hinders the process [77]. The rate of formation of NiO NPs is higher in basic pH than in acidic pH. The formation of NiO NPs occurs rapidly in the basic pH, it may be due to the ionization of the phenolic group present in the extract. The slow rate of formation and aggregation of NiO NPs at acidic pH could be related to the electrostatic repulsion of anions present in the solution [70] (appendix figure 32).

### The volume of dopant for nanocomposites.

The absorption peak of Cu-NiO NCs was also affected by the concentration of dopant [78]. To see the effect of dopant (Cu) on the synthesis of Cu-NiO NCs; the different volume of dopant (0.1M Cu (NO)<sub>2</sub>. 3H<sub>2</sub>O) was added to get the optimum volume of the reaction. These are 10% (5mL), 20% (10 mL), 30% (15 mL), 40% (20 mL), and 60% (30 mL). Finally, 20% was optimized since it gave UV-Vis absorbance value at the largest wave length (red shift).

Therefore, it is possible to form a large amount of highly dispersed NPs with small particle sizes using P. d leaf extracts efficiently both as a reducing and stabilizing agent. The proposed mechanism metal (II) ion, i.e. Ni<sup>2+</sup> based nanostructure like NiO is given in figure 16 as stated by literature [4].

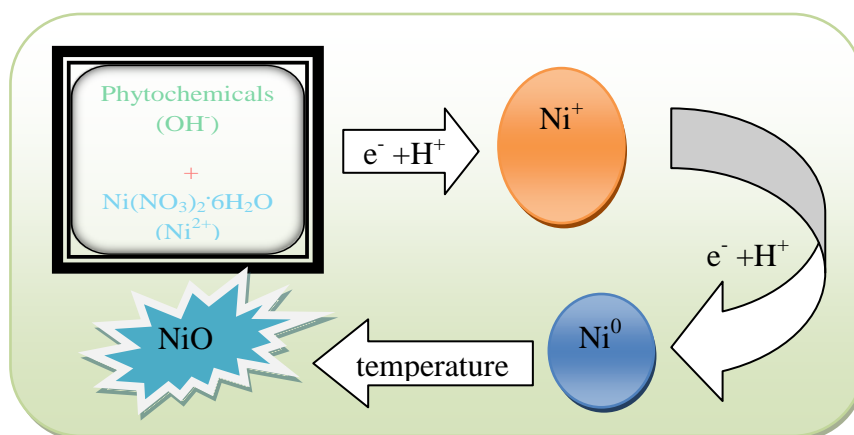


Figure 16. The chemical reaction for the synthesis of NiO NPs in the presence of plant extract.

### 4.3. Characterization of the synthesized samples.

#### 4.3.1. Electronic spectra of the synthesized nanoparticles

The synthesized NiO NPs and Cu-NiO NCs were characterized by UV-Vis spectroscopy. UV-Vis spectroscopy is one of the most widely used simple and sensitive techniques for the identification of nanoparticles formation.

The UV-Vis spectra of the NPs and NCs were recorded in the range of 300-700 nm at room temperature. The obtained NPs displayed the characteristic surface Plasmon resonance (SPR) band in the spectral range of 350-356 nm. This was in line with the study conducted by literature [23] that report optimum absorbance of NiO NPs at 350 nm wave length. The optimized NiO and Cu-NiO NCs were resulted by giving maximum UV-Vis absorbance at 350 and 356 nm respectively as shown in figure 17. This figure is consistent with a recently reported study [48].

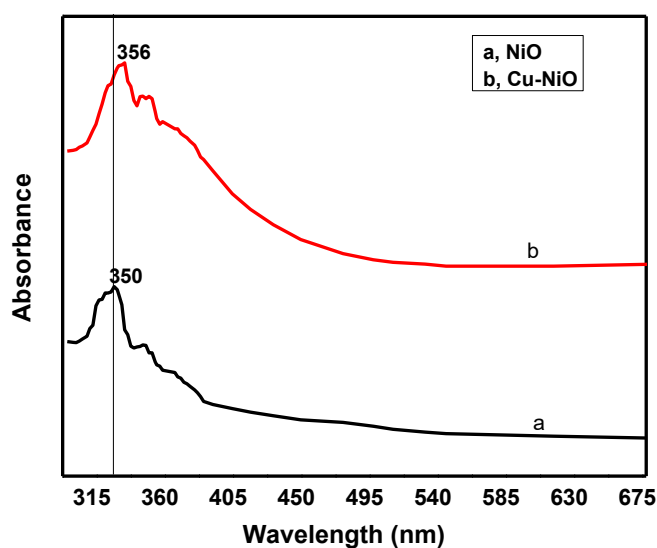


Figure 17. UV-Vis spectra of NiO NPs and Cu-NiO NCs

The Tauc's plot is shown in figure 18. The optical band gap for the absorption peak is obtained by extrapolating the linear portion of  $(\alpha h\nu)^2$  versus  $h\nu$  to zero.  $E_g$  was found to be 3.19 eV and 2.85 eV for NiO NPs and copper doped NiO NCs respectively. The Cu-NiO NCs exhibit lower bandgap energy than NiO NPs.

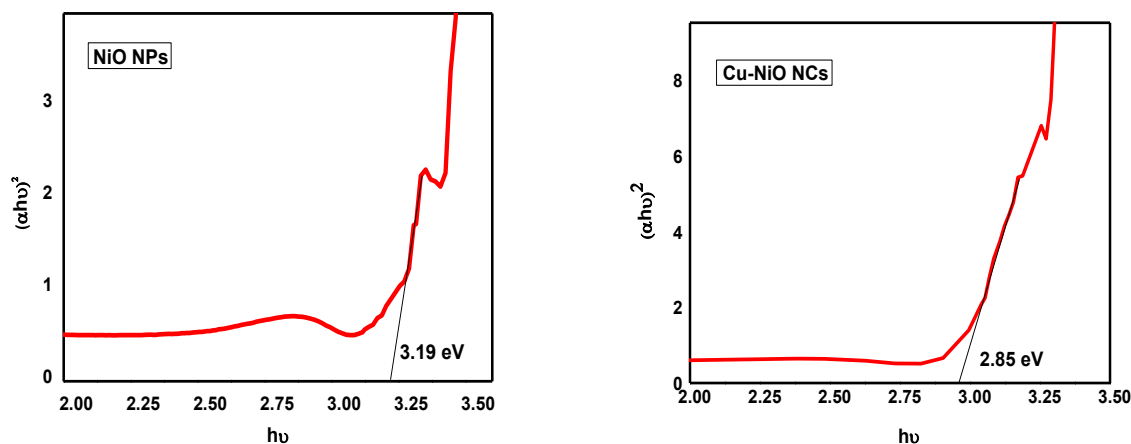


Figure 18. The calculated band gap of the synthesized samples

#### 4.3.2. Fourier transform infrared (FT-IR) spectroscopy

The FTIR spectrum of leaf extract showed multiple peak values indicating the presence of phenols, alcohols, alkanes, alkenes, aromatic compounds, carboxylic acid, and alkyl halides (figure 19). The absence of peaks at  $2220\text{--}2260\text{ cm}^{-1}$  indicated the absence of cyanide derivatives [58]. The absorption bands at  $471\text{ cm}^{-1}$  are attributed to Ni-O vibrations [62] (figure 20). In the case of Cu doped NiO NCs in addition to the  $469\text{ cm}^{-1}$  peak due to Ni-O stretching the  $631\text{ cm}^{-1}$  band was observed which indicated the Cu-O stretching vibration band (figure 20). The other peaks at  $1051\text{ cm}^{-1}$  seen in the doped sample can be assigned to the different modes of Cu-O bond bending vibrations which are in good agreement with the reported literature [79].

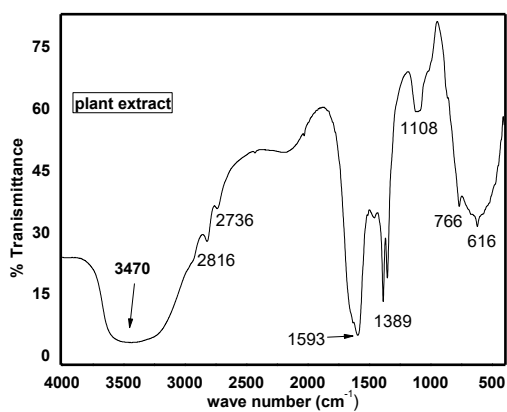


Figure 19. The FT-IR spectrum of pure Phytolacca dodecandra l'herit leaves extract.

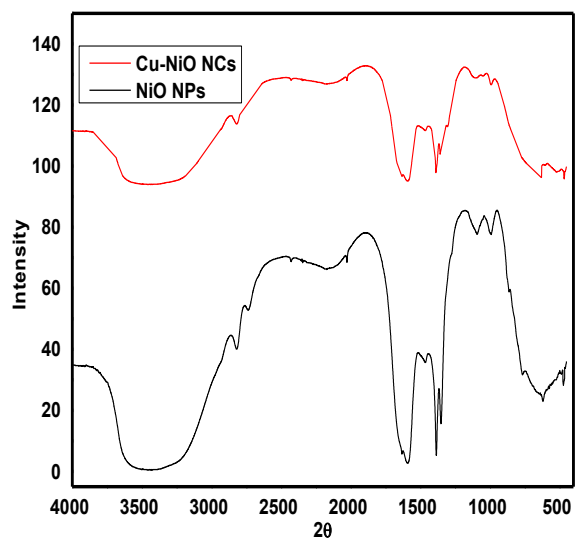


Figure 20. The FT-IR spectrum of the synthesized NiO NPs and Cu-NiO NCs.

From figure 19 and 20, the very strong absorption band observed around  $3400\text{ cm}^{-1}$  may be due to the presence of bonded N–H/C–H/O–H stretching of amines, amides, and alcohols. These peaks are consistent with the earlier reported spectra [80] and [81] because this plant leaf contains phenolic and alkaloids phytochemicals.



Table 3. FT-IR spectral peak values and functional groups of the plant extracts, NiO NPs and Cu-NiO NCs.

Type of graph	Peak value	Bond	Vibration	Functional group	Reference
	616	C-H	Wagging	Alkynes	[82, 83]
	766	C-Br/Cl	Stretch	Alkyl halides	[39, 83]
<b>Plant extract</b>	1108	C-O	-	Carboxylic acid, alcohol	[58]
	1351	C-H	-	Aromatic	[84]
	1385	-	-	Nitrates	[39]
	1593	N-H	Deformation	Secondary amine	[82]
	2027	C-H	-	Aliphatic	[84]
	2736	C-H	Stretching	Alkyl	[39]
	2820	C-H	Stretching	Alkane	[85]
	3470	H-bonded	stretching,	Phenols, alcohol	[82]
<b>NiO</b>	471	Ni-O	Wagging	-	[84, 86]
	618	Ni-O	Stretching	-	[84]
	991	Ni-OH	Heavy vibration	-	[84]
	1351	C-H	-	Aromatic	[84]
	1385	-	-	Nitrates	[39]
	1585	-	Deformation	Secondary amine	[82]
	3463	H-bonded	stretching,	Phenols, alcohol	[82]
<b>Cu-NiO</b>	467	Ni-O	Wagging	-	[84, 86]
	604	Ni-O	Stretching	-	[84]
	631	Cu-O	Stretching	-	[79]
	991	Ni-OH	Heavy vibration	-	[84]
	1051	Cu-OH	Bending	-	[79]
	3454	H-bonded	stretching,	Phenols, alcohol	[82]

### 4.3.3. X-ray diffraction (XRD) analysis.

The crystallinity and crystalline phase of synthesized samples were determined through X-ray diffraction (XRD) profiles (DR AWELL XRD -700 using  $2\text{CuK}\alpha$  radiation) in  $2\theta$  range of  $20^\circ$  to  $80^\circ$  with a scan speed of  $0.03^\circ/\text{min}$ . The XRD pattern of NiO NPs and Cu-NiO NCs is shown in Figure 21. XRD pattern reveals the face-centered cubic structured NiO. The Bragg peaks were obtained at  $2\theta$  values of  $37.46^\circ$ ,  $43.51^\circ$ ,  $63.16^\circ$ ,  $75.65^\circ$ , and  $79.71^\circ$  degrees corresponding to (111), (200), (202), (311), and (222) respectively. We have not detected any other additional peaks throughout this diagram, which confirms the purity of obtained nanoparticles. The gathered data has been following the standard pattern (JCPDS # 96-101-0096). All the reflection can be indexed to face-centered cubic NiO phase, similarly with recently reported works of literature [87, 88]

The diffraction peaks are found to broaden up with decrement in their intensity as copper is doped in NiO which may be microstructural strain produced by the introduction of  $\text{Cu}^{+2}$  ions in NiO lattice [62]. The crystallite size was found to increase with the doping of copper in nickel oxide due to the difference in ionic radii of copper and nickel ion. It is clear from figure 21, that no other characteristic peak due to any impurities and sharp peaks are present in the pattern, indicating that the prepared samples are of high purity and crystallinity. The Bragg peaks were obtained at  $2\theta$  values of  $35.74^\circ$ ,  $37.37^\circ$ ,  $43.35^\circ$ ,  $48.87^\circ$ ,  $62.96^\circ$ ,  $68.34^\circ$ ,  $75.28^\circ$ , and  $79.51^\circ$  degree correspond to (11-1), (111), (200), (20-2), (202), (110), (311), and (222) respectively. The gathered data has been following the standard pattern (JCPDS # 96-901-4581). The additional peaks obtained at  $35.74^\circ$ ,  $48.87^\circ$ , and  $68.34^\circ$  correspond to copper, this is identical with reported literature [89]. XRD of copper doped NiO can have a pattern related to the presence of copper as revealed by literature [90].

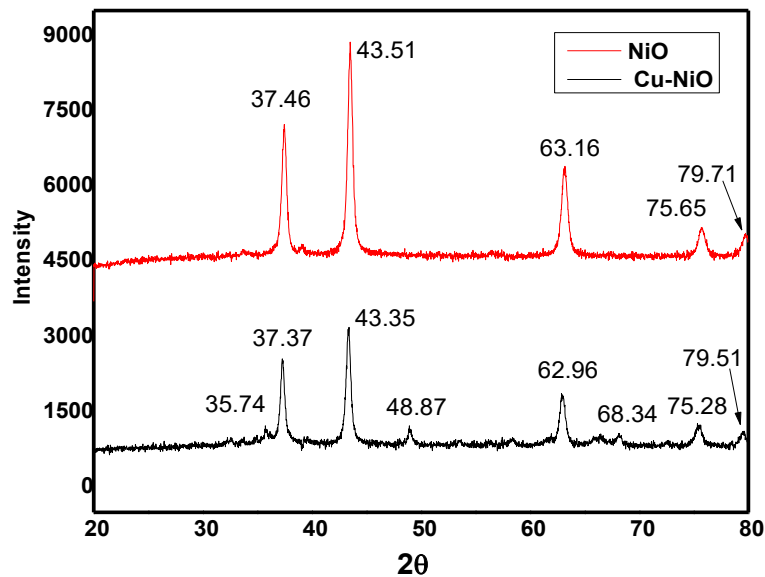
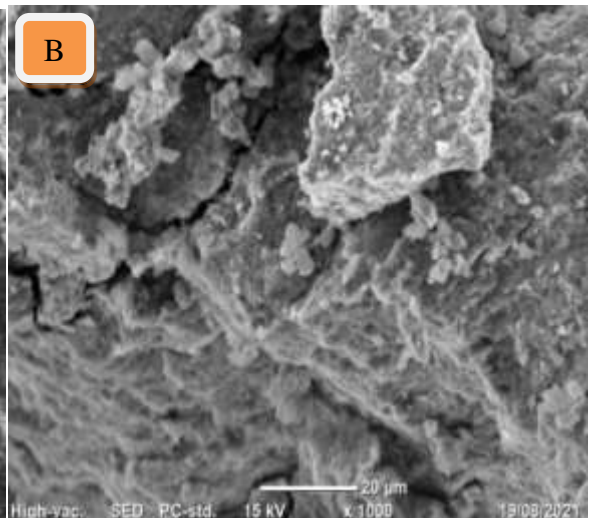
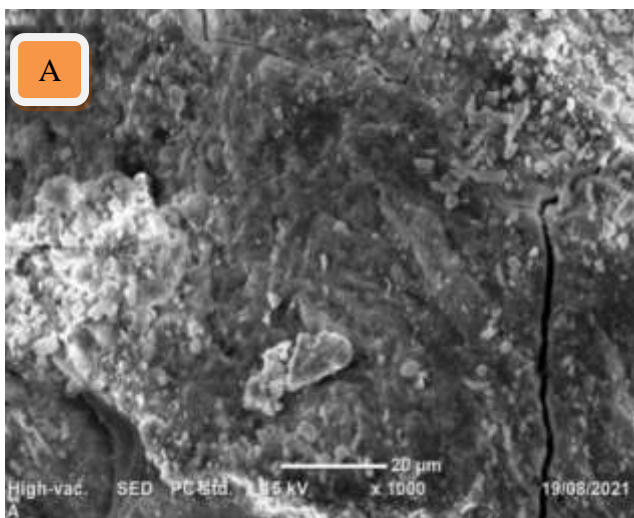
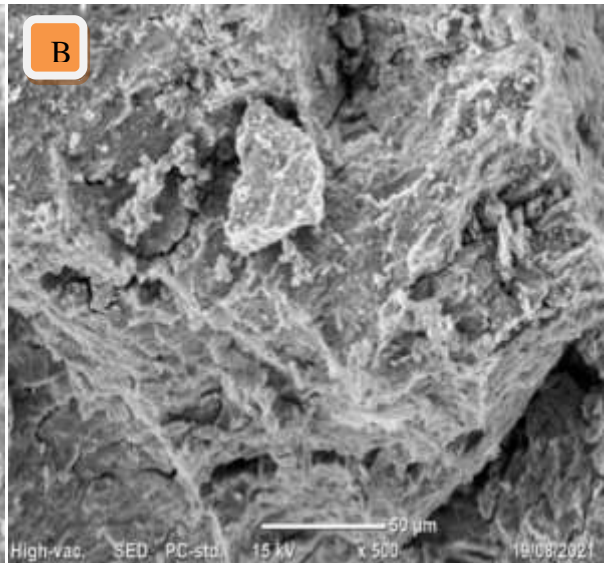
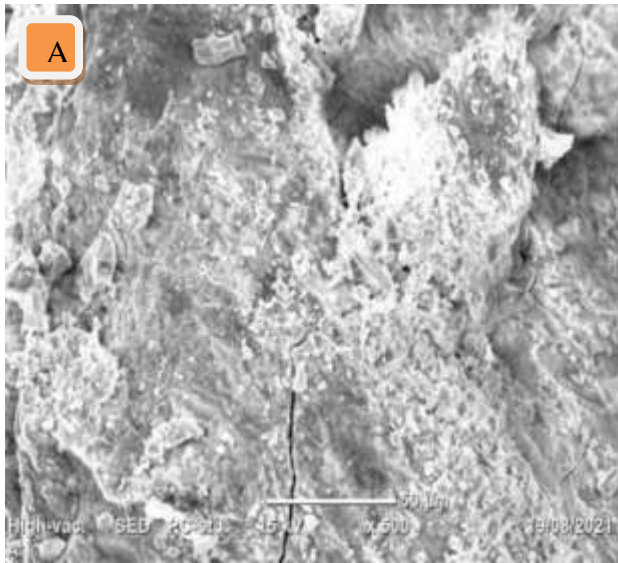
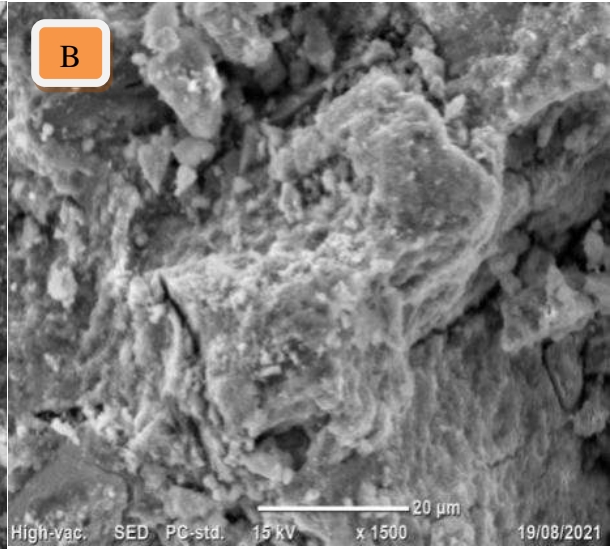
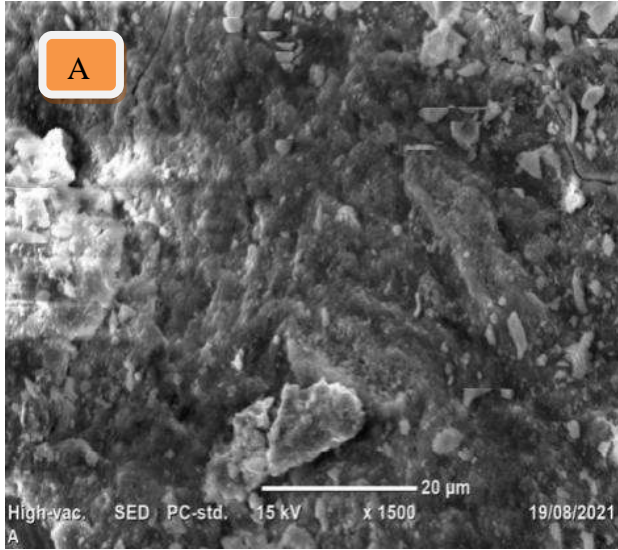


Figure 21. X-ray pattern of NiO NPs and Cu-NiO NCs.

The average size of the synthesized NiO NPs and Cu-NiO NCs was calculated by using Scherrer's formula from data of X-ray diffraction (XRD) pattern is 14.18 and 16.10 nm respectively. The crystallite size was found to increase with the doping of Cu in NiO because the ionic radius of Cu is bigger than Ni (Cu = 0.082 nm > Ni = 0.078 nm) [91, 92].

#### 4.3.4. Scanning Electron Microscopy (SEM) analysis

The surface morphological features of synthesized pure and doped NiO samples were studied by scanning electron microscope; the images were recorded with the magnification of 1500, 1000, 500, and 50 (Figure 22). SEM results demonstrate that they are appropriately dispersed and particles are cubical and are highly crystalline (< 10 nm), This is in good agreement with reported literature [93]. Both the samples were showing nearly the same morphological features. Some of the synthesized nanoparticles are found agglomerated due to aggregating or overlapping of smaller particles and they are essentially a cluster of nanoparticles, which is closely consistent with the result in literature [94] that found an average size distribution of about 18 nm. It can be seen that pure NiO NPs reveal smaller-sized particles, while the doped sample shows comparatively large-sized particles. This result is in good agreement with the XRD data which showed the formation of larger particle sizes in Cu doped NiO NCs.



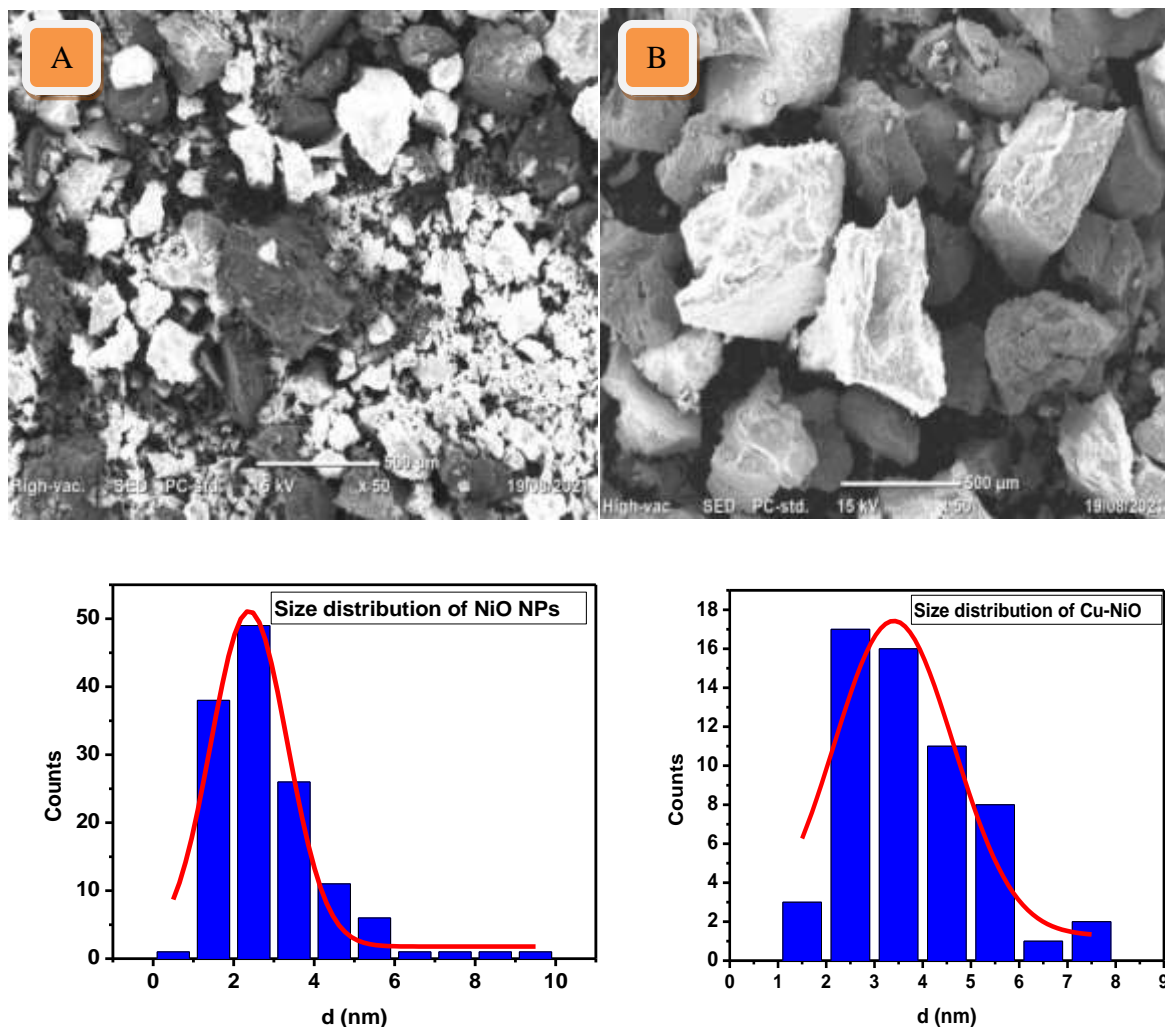


Figure 22. SEM images of NiO (a), Cu-NiO (b), and their size distributions (20  $\mu\text{m}$ , 1000 mag.).

#### 4.4. Photocatalytic Degradation of Dye

##### 4.4.1. Effect of pH of the solution.

The pH of reaction media has been known as the one feature that decides the Photocatalytic proficiency of the catalyst. The Photocatalytic ability of synthesized NiO NPs was analyzed against the different pH of MB solution. The pH of the solution was adjusted by using 0.1 M NaOH and 0.1 M HCl. The Photocatalytic ability of the synthesized NiO NPs is directly proportional to the pH of the dye solution. Therefore, as the pH of the dye solution increases from 8 to 11, the degradation of MB dye also increases (Figure 23). The reason here is the variation of pH alters the surface properties of NiO NPs. The pHPZC (pH at point of zero

charges) of Cu-NiO NCs was estimated at 6.98 (appendix figure 31). At pHPZC catalysts has net-zero charges and at  $\text{pH} < \text{pHPZC}$  the surface of a catalyst becomes positively charged. Whereas at  $\text{pH} > \text{pHPZC}$  the surface is negatively charged. MB is a cationic dye, hence at  $\text{pH} < \text{pHPZC}$  displayed repulsive behavior due to a positively charged surface of the catalyst. Therefore degradation proficiency decreases. When  $\text{pH} > \text{pHPZC}$  the catalyst surface has a negative charge which attracts the MB dye molecules to a greater extent [6].

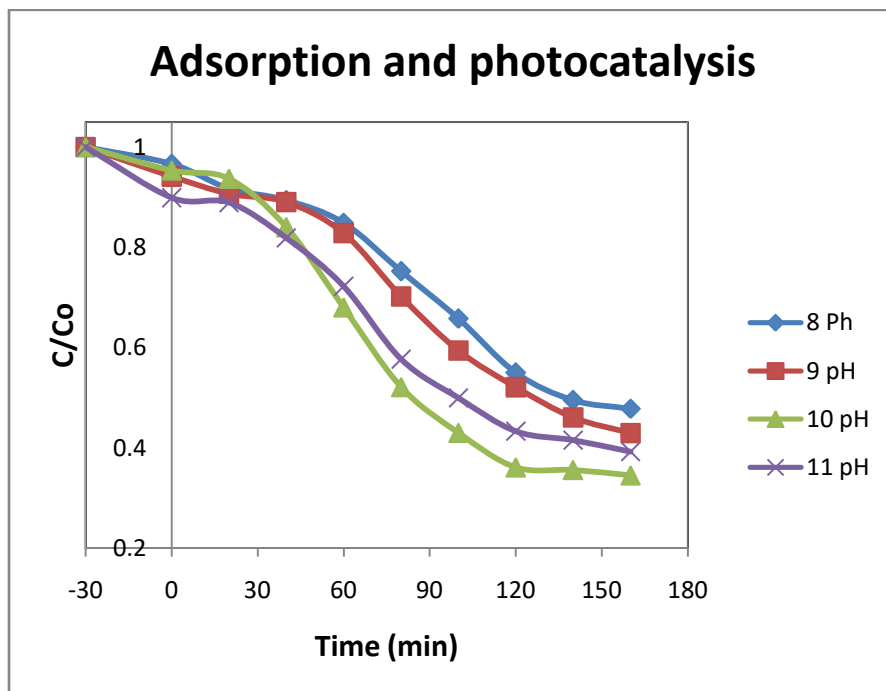


Figure 23. Effect of pH on MB removal with catalyst.

The experiment was carried out in the presence of NiO NPs and Cu-NiO NCs for irradiation time of 160 min at 10 mg/L dye concentration as shown in Figure 23. At pH 10 per hydroxyl, radicals are formed, leading to the formation of hydrogen peroxide which offers rise to hydroxyl radicals on a large scale. This increases the Photocatalytic proficiency of catalysts under sunlight irradiation and the degradation of MB dye reaches up to 97.8%. At  $\text{pH} = 11$ , the surface of the catalyst becomes negatively charged by metal-bound  $\text{OH}^-$ , as a result the adsorption of MB molecules is hindered and becomes less available for degradation, due to the electrostatic repulsion between the surface charges on the adsorbate and the adsorbent and so a decreased photocatalytic degradation efficiency was observed, this is in good agreement with recently reported literature [59].

#### 4.4.2. Effect of initial dye concentration.

For determining the effect of dye concentration on the degradation ability of the catalyst. The experiment was carried out at an optimized pH and irradiation time of 160 min by changing the initial dye concentration of 7, 10, and 13 mg/L. The MB solution containing NPs was kept in dark for 30 min to achieve the adsorption-desorption equilibrium. The percent removal of MB solutions ranging from 7, 10, to 13 mg/L was found to be around 10%–15% after the 30 min adsorption in dark. Then it was followed by Photocatalytic degradation under the UV-Vis light irradiation by assuming the time  $t = 0$ . Figure 24, clearly shows the degradation proficiency of the catalyst is inversely relative to the initial dye concentration of MB dye. As the initial dye concentration of MB increases, the time needed for complete degradation is increasing and Photocatalytic proficiency decreases. At a high concentration of a dye maximum number of dye molecules adsorbed on the catalyst surface resulting in reduced light penetration. Due to this lesser number of hydroxyl and hence Photocatalytic activity diminished, this is also reported in the literature [3].

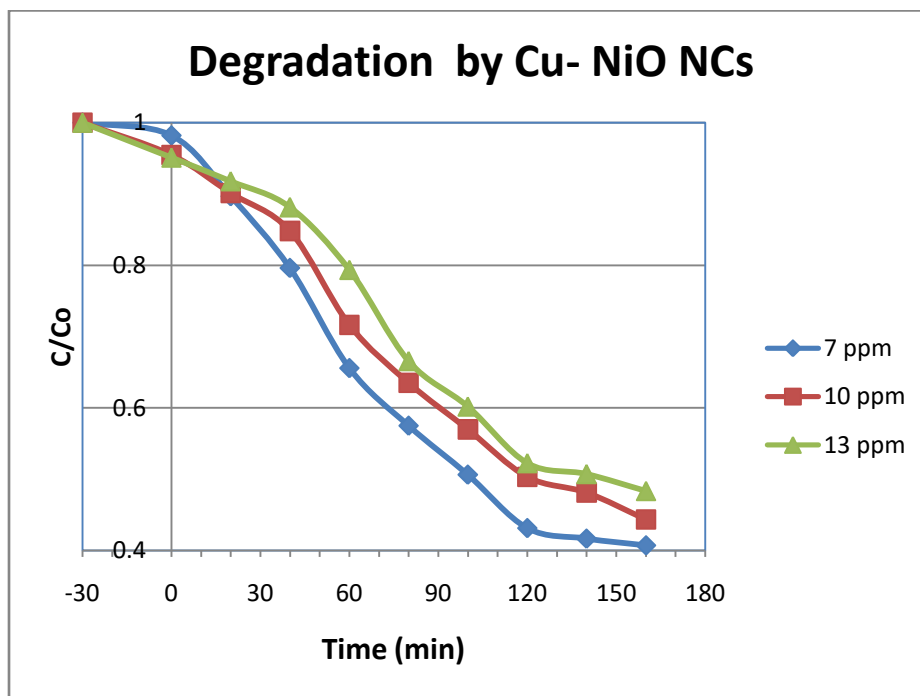


Figure 24. Effect of initial dye concentration on photocatalytic degradation.

#### 4.4.3. Effect of irradiation time.

The reaction kinetics depends on the irradiation time, hence a suitable length of time is necessary to achieve the best results [92]. The relationship between degradation proficiency of catalyst for MB dye degradations and contact time was examined at the optimized condition of MB at pH 10 dye concentrations of 10 mg/L and catalyst dose 0.6 gm/L. The results are shown in Figure 26. The degradation of MB has shown regular reduction with increasing the irradiation time under sunlight. The decolorization of the dye solution took place in 160 min of irradiation (Appendix Figure 32). The corresponding degradation proficiency of MB was found to be 78.3 and 97.8% by NiO NPs and Cu-NiO NCs respectively. The blank (photolysis) which was insignificant also shown in figure 25.

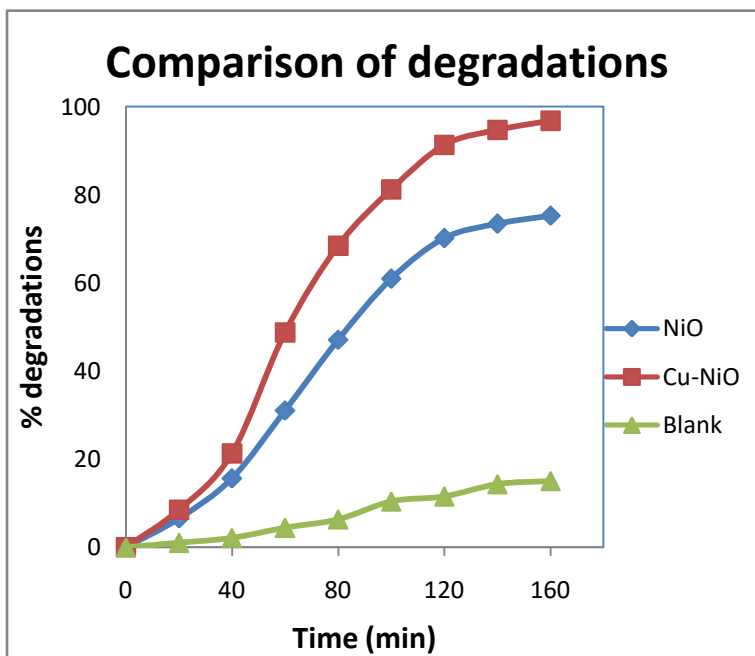


Figure 25. Comparison of degradation of MB by sunlight with and without catalysts.

#### 4.4.4. Effect of catalyst dose.

The effect of photocatalyst mass was studied on dye degradation keeping other experimental conditions constant. The percentage degradation of MB was studied under different concentrations of catalysts amount in the range of 20 – 60 mg at a constant dye concentration of 10 mg/L, which is in line and lower in dose with the literature [95]. The number of photons absorbed and the number of dye molecules degraded were increased with the increase in catalyst



concentration [3]. The photocatalytic activity goes on increasing with catalytic load due to the uniform dispersion of catalyst and the availability of a more active site on the surface of the catalyst [6]. Similarly, it is observed that the initial rate increases with the increase in catalyst concentration as shown in Figure 26.

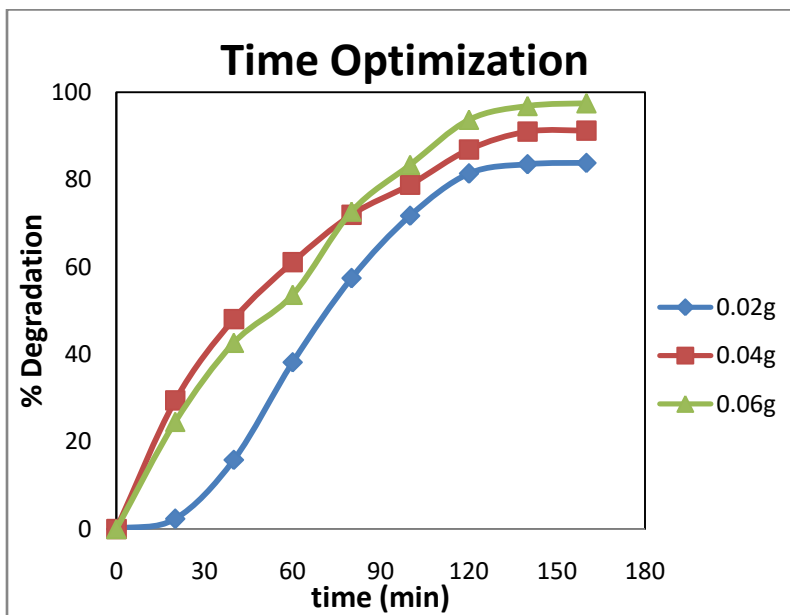


Figure 26. Effect of irradiation time and catalyst dose on Photocatalytic degradation

#### 4.4.5. Reusable performance of the nanoparticles.

Figure 27, shows that the removal of the MB by the NiO NPs and Cu-NiO NCs photocatalysts after the 1st run achieved up to 65.08% and 70.99% respectively. After the 2nd run, the removal of the MB decreases down to 41.81 and 55.42%. The decrease in the removal of the MB is probably due to the loss of the recycled catalyst during sampling. Figure 27 shows that NiO NPs and Cu-NiO NCs have excellent stability and do not suffer from photo-corrosion during degradation, this is in line with reported literature [3].

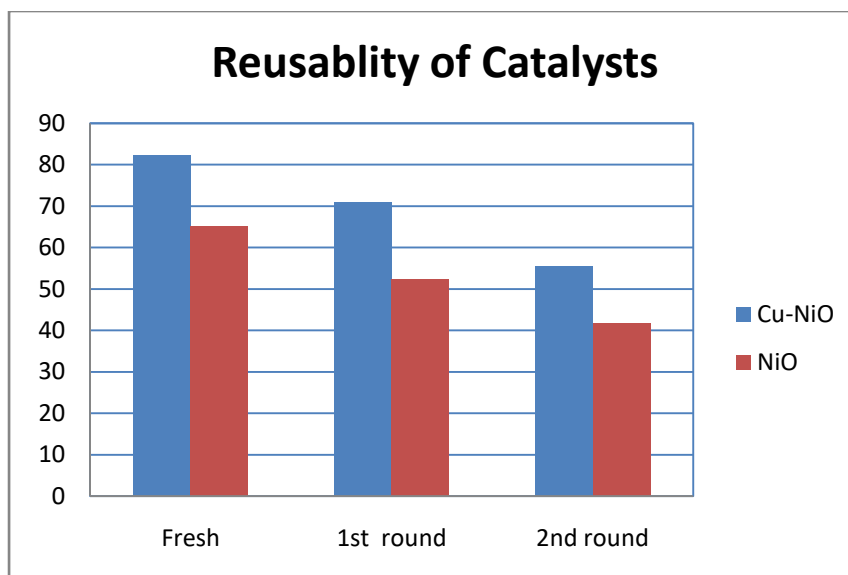


Figure 27. Recycling performance of particles.

#### 4.5. Antioxidant activity

Antioxidants were characterized by the capacity to scavenge free radicals and major aspect of antioxidants is the ability to donate hydrogen or electron to the oxidants [6]. The scavenging activities of the particles were estimated using the following concentrations: 1000, 750, 500, 250, 100, and 50  $\mu\text{g/mL}$ . The results (Figure 28) showed the effective free radical scavenging activity of the synthesized samples compared to Ascorbic acid (302.74  $\mu\text{g/mL}$ ), with calculated  $\text{IC}_{50}$  values of 350.29 and 363.96  $\mu\text{g/mL}$  for Cu-NiO NCs and NiO NPs respectively, which is in line with the literature [96] that was reported as  $\text{IC}_{50}$  of 339  $\mu\text{g/mL}$  by Biosynthesis of iron oxide ( $\text{Fe}_2\text{O}_3$ ) nanoparticles. Similarly, the hydroxyl radical scavenging activity of NiO NPs ( $\text{IC}_{50}$  value is 329.20  $\mu\text{g/mL}$ ) was reported in the literature [6]. The  $\text{IC}_{50}$  values demonstrate the ability to inhibit radicals. The result may be due to the presence of Polyphenols. Phenols are the most common secondary metabolites in the plant kingdom. They have numerous biological properties including antioxidant capacities for which they are indicated in the management of several diseases [97].

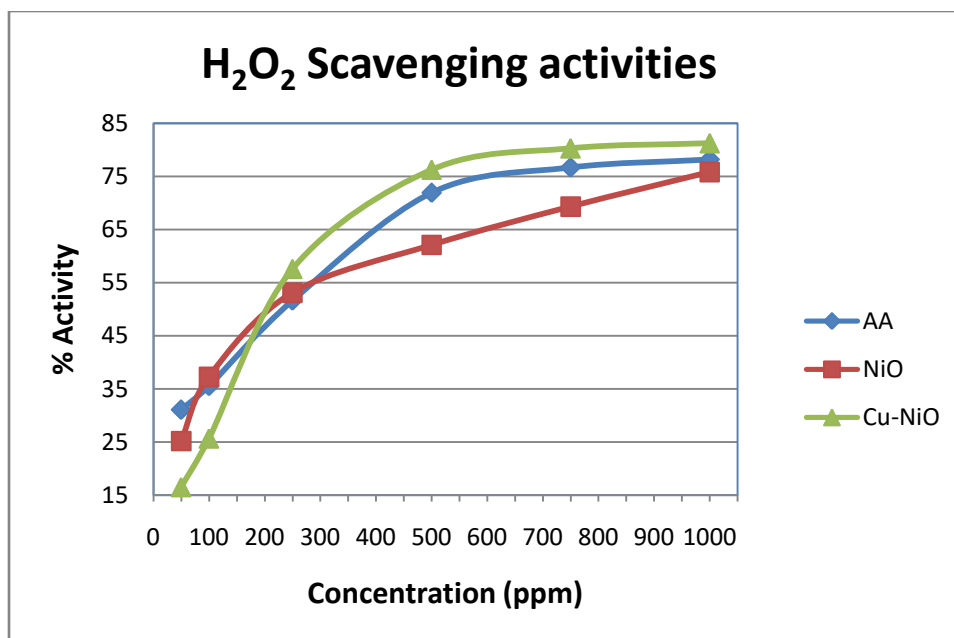


Figure 28. Antioxidant activities of biogenically synthesized NPs and AA.

Enhance in the antioxidant activity of the biosynthesized NiO NPs might be an effect of metal ions present in the particles; the possible predicted mechanism is illustrated in Figure 29. It has been reported that enzymes utilizing metal ion (Zn) as a cofactor scavenge H<sub>2</sub>O<sub>2</sub> free radicals [98]. In this study, the presence of Ni and Cu ions in particles might be responsible for higher H<sub>2</sub>O<sub>2</sub> free radical scavenging activity. The hydroxyl radical scavenging potential of NCs was found to be more significant than NPs.

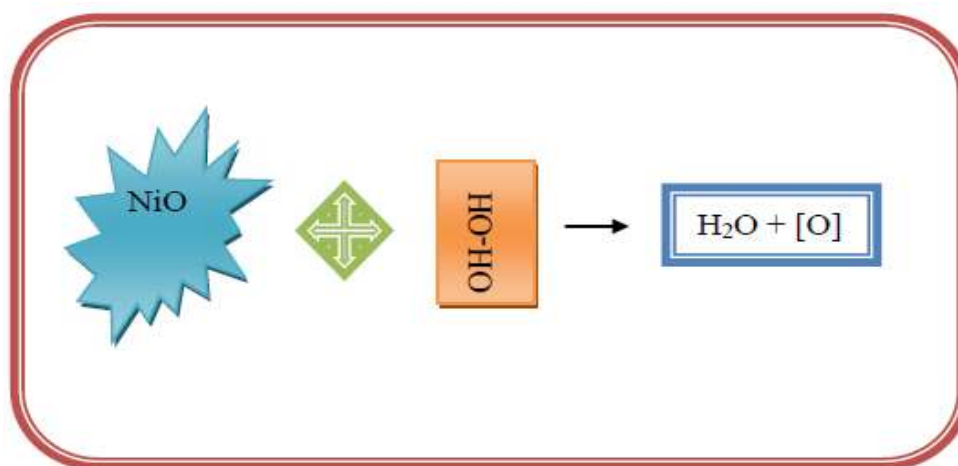


Figure 29. Predicted mechanism of H<sub>2</sub>O<sub>2</sub> scavenging activity.

## 5. CONCLUSION AND RECOMMENDATION

### 5.1. Conclusion

In general, a simple, clean, economically viable, and green approach has been established for the synthesized NiO NPs and Cu-NiO NCs by using *Phytolacca dodecandra l'herit* leaf extract as a reducing and capping agent. The UV-Vis absorption peaks at 350 and 356 nm indicate the synthesis of NiO NPs and Cu-NiO NCs respectively. FT-IR studies confirmed the biofabrication of the NPs by the action of different phytochemicals with its different functional groups present in the leaves extract. The XRD patterns confirmed the purity, phase composition, and crystalline nature of the synthesized nanoparticles. XRD pattern showed distinctive peaks corresponding to (111), (200), (202), (311), and (222) planes that can be indexed as the typical face-centered cubic structure. Crystalline sizes of the formed particle were obtained to be 14.18 and 16.10 nm from the XRD data by using Scherrer's formula for NiO NPs and Cu-NiO NCs respectively. SEM results also demonstrate that particles are appropriately dispersed, cubical, and highly crystalline with a size of less than 10 nm.

The designed nanoparticles are highly stable and have shown significant Photocatalytic and antioxidant activities against Methylene blue degradation and Hydrogen peroxide scavenging. The Photocatalytic degradation of Methylene blue (MB) was found to be 78.3 and 97.8% by NiO NPs and Cu-NiO NCs respectively. In the antioxidant test, NiO NPs and Cu-NiO NCs prevented the oxidation of 50% of the H<sub>2</sub>O<sub>2</sub> molecules at a concentration of 363.96 µg/mL and 350.29 µg/mL respectively. Considering the obtained results, NiO NPs and Cu-NiO NCs containing *Phytolacca dodecandra l'herit* leaf aqueous extract may be utilized as an efficient drug/supplement in treating diseases in humans after sufficient clinical studies. From the photocatalytic studies, the synthesized samples are found to be promising photocatalysts in the abatement of organic pollutants.

### 5.2. Recommendation

The advanced study should be carried out using other characterization techniques of compounds acting as the reducing agents in plant extract and Nanoparticles which were not addressed by this study. Also, anti-oxidant activity of the synthesized samples should be compared with the leaf extract.

## 6. REFERENCES

- [1] Imran Din, M.; Rani, A. Recent Advances in the Synthesis and Stabilization of Nickel and Nickel Oxide Nanoparticles: A Green Adeptness. *Int. J. Anal. Chem.*, **2016**.
- [2] Mohana, S.; Elango, G.; Priya, D. D.; Asharani, I. V.; Kishore, B. Sunlight Mediated Photocatalytic Degradation of Organic Pollutants by Statistical Optimization of Green Synthesized NiO NPs as Catalyst. *J. Mol. Liq.*, **2019**, 293, 111509.
- [3] Khairnar, S. D.; Shrivastava, V. S. Facile Synthesis of Nickel Oxide Nanoparticles for the Degradation of Methylene Blue and Rhodamine B Dye: A Comparative Study. *J. Taibah Univ. Sci.*, **2019**, 13, 1108–1118.
- [4] Haq, S.; Dildar, S.; Ali, M. Ben; Mezni, A.; Hed, A.; Shahzad, M. I. Antimicrobial and Antioxidant Properties of Biosynthesized of NiO Nanoparticles Using Raphanus Sativus ( R . Sativus ) Extract. **2021**.
- [5] Khalil, I.; Yehye, W. A.; Etxeberria, A. E.; Alhadi, A. A.; Dezfooli, S. M.; Binti, N.; Julkapli, M. Nanoantioxidants : Recent Trends in Antioxidant Delivery Applications.
- [6] Kumar, M. S. S.; Soundarya, T. L.; Nagaraju, G.; Raghu, G. K.; Rekha, N. D.; Alharthi, F. A.; Nirmala, B. Multifunctional Applications of Nickel Oxide ( NiO ) Nanoparticles Synthesized by Facile Green Combustion Method Using Limonia Acidissima Natural Fruit Juice. *Inorganica Chim. Acta*, **2020**, 120059.
- [7] Hussain, A. F. uv-visible spectrometry. **2019**.
- [8] Habtemariam, A. B. Plant Extract Mediated Synthesis of Nickel Oxide Nanoparticles. **2020**, 2, 205–209.
- [9] Getu, Z. Green Synthesis and Nanoparticles Using Endod ( Phytolaccadodecandra ) Leaf Extract and Evaluation Of anti-microbial activities. **2019**.
- [10] Tolesa, A. Chemical and Biological Synthesis of Cobalt Oxide Nanoparticles: Comparative Study of Antibacterial Activity. Ethiopia. **2019**.
- [11] Srihasam, S.; Thyagarajan, K.; Korivi, M.; Lebaka, V. R.; Mallem, S. P. R. Phytogetic Generation of NiO Nanoparticles Using Stevia Leaf Extract and Evaluation of Their In-Vitro Antioxidant and Antimicrobial Properties. *Biomolecules*, **2020**, 10.
- [12] Khalil, A. T.; Ovais, M.; Ullah, I.; Ali, M.; Khan, Z.; Hassan, D.; Maaza, M.; Talha, A.; Ovais, M.; Ullah, I.; et al. Sageretia Thea ( Osbeck .) Modulated Biosynthesis of NiO Nanoparticles and Their in Vitro Pharmacognostic , Antioxidant and Cytotoxic Potential. *Artif. Cells, Nanomedicine, Biotechnol.*, **2018**, 838–852.
- [13] Jeba, D. P.; Amaladhas, T. P. Green Synthesis and Photocatalytic Activity of Nickel Oxide Nanostructures in the Degradation of Organic Dyes. *Int. J. Res. Advent Technol.*, **2018**, 6.

- [14] Ash, F. Y.; Induc, L.; Strat., O. R. S. Green Synthesis and Photocatalytic Activity of Nickel Oxide Nanostructures in the Degradation of Organic Dyes. **2018**.
- [15] Xavier, S.; Lakshmi, V.; Jenila, R. M. EPRA International Journal of Research and Development ( IJR D ) synthesis of nio nanoparticles using thespesia populnea leaves by green. **2019**, 7838.
- [16] Peralta-vidua, J. R.; Huang, Y.; Parsons, J. G.; Zhao, L. Plant-Based Green Synthesis of Metallic Nanoparticles: Scientific Curiosity or a Realistic Alternative to Chemical Synthesis. *Nanotechnol. Environ. Eng.*, **2016**, 1, 1–29.
- [17] Claudel, M.; Schwarte, J. V.; Fromm, K. M. New Antimicrobial Strategies Based on Metal Complexes. *Chemistry (Easton)*., **2020**, 2, 849–899.
- [18] Mahaleh, Y. B. M.; Sadrnezhaad, S. K.; Hosseini, D. NiO Nanoparticles Synthesis by Chemical Precipitation and Effect of Applied Surfactant on Distribution of Particle Size. **2008**.
- [19] Arun, L.; Karthikeyan, C.; Philip, D.; Unni, C. Journal of Physics and Chemistry of Solids Optical , Magnetic , Electrical , and Chemo-Catalytic Properties of Bio- Synthesized CuO / NiO Nanocomposites. *J. Phys. Chem. Solids*, **2020**, 136, 109155.
- [20] Sachdeva, H.; Dwivedi, D.; Bhattacharjee, R. R.; Khaturia, S.; Saroj, R. NiO Nanoparticles : An Efficient Catalyst for the Multicomponent One-Pot Synthesis of Novel Spiro and Condensed Indole Derivatives. **2013**.
- [21] Nescu, A. C. O. M. Ă.; Mihaly, M.; Meghea, A. Photocatalytic Degradation of Organic Pollutants Using NiO Based Materials photocatalytic degradation of organic pollutants using nio based materials. **2012**.
- [22] Kaur, N.; Singh, J.; Kaur, G.; Kumar, S.; Kukkar, D.; Rawat, M. CTAB Assisted Co-Precipitation Synthesis of NiO Nanoparticles and Their Efficient Potential towards the Removal of Industrial Dyes. **2019**.
- [23] Haider, A.; Ijaz, M.; Ali, S.; Haider, J.; Imran, M.; Majeed, H.; Shahzadi, I.; Ali, M. M.; Khan, J. A.; Ikram, M. Green Synthesized Phytochemically ( Zingiber Officinale and Allium Sativum ) Reduced Nickel Oxide Nanoparticles Confirmed Bactericidal and Catalytic Potential. **2020**.
- [24] Anitha, C.; Sumathi, S.; Tharmaraj, P.; Sheela, C. D. Synthesis, Characterization, and Biological Activity of Some Transition Metal Complexes Derived from Novel Hydrazone Azo Schiff Base Ligand. *Int. J. Inorg. Chem.*, **2011**, 2011, 1–8.
- [25] Adinaveen, T.; Karnan, T.; Arul, S.; Selvakumar, S. Heliyon Photocatalytic and Optical Properties of NiO Added Nephelium Lappaceum L . Peel Extract: An Attempt to Convert Waste to a Valuable Product. *Heliyon*, **2019**, 5, 01751.
- [26] Ahmad, Z.; Afzal, A. M.; Khan, M. F.; Manzoor, A.; Khalil, H. M. W.; Aftab, S. Copper-Doped Nickle-Oxide Nanoparticles for Photocatalytic Degradation of Erichrome Black-T and Methylene

- Blue and Its Solar Cell Applications. **2019**, 1–9.
- [27] Mohammadijoo, M.; Sadrnezhad, S. K.; Mazinani, V. Synthesis and Characterization of Nickel Oxide Nanoparticle with Wide Band Gap Energy Prepared via Thermochemical Processing *Nanoscience and Nanotechnology : An International Journal ISSN* **2014**, 4–8.
- [28] Oyeyemi, I. T.; Akinlabi, A. A.; Adewumi, A.; Aleshinloye, A. O. Vernonia Amygdalina : A Folkloric Herb with Anthelmintic Properties Beni-Suef University Vernonia Amygdalina , *Beni-Suef Univ. J. Basic Appl. Sci.*, **2017**.
- [29] Nagajyothi, P. C.; Vattikuti, S. V. P.; Devarayapalli, K. C.; Yoo, K.; Sreekanth, T. V. M.; Vattikuti, S. V. P.; Devarayapalli, K. C.; Yoo, K. Technology Green Synthesis : Photocatalytic Degradation of Textile Dyes Using Metal and Metal Oxide Nanoparticles-Latest Trends and Advancements Green Synthesis : *Crit. Rev. Environ. Sci. Technol.*, **2019**, 1–107.
- [30] Patra, J. K.; Baek, K. H. Green Nanobiotechnology: Factors Affecting Synthesis and Characterization Techniques. *J. Nanomater.*, **2014**.
- [31] Ruth, O.; Hamid, N.; Kholijah, S.; Mudalip, A. phytochemical and pharmacological properties of Vernonia Amygdalina : A review. **2017**, 2, 80–96.
- [32] Dye, O. Synthesized and Photocatalytic Mechanism of the NiO Supported YMnO<sub>3</sub> Nanoparticles for Photocatalytic Degradation of the Methylene blue. Introduction. **2019**.
- [33] Altemimi, A.; Lakhssassi, N.; Baharlouei, A.; Watson, D. G.; Lightfoot, D. A. Phytochemicals: Extraction, Isolation, and Identification of Bioactive Compounds from Plant Extracts. *Plants*, **2017**, 6 .
- [34] Angel Ezhilarasi, A.; Judith Vijaya, J.; Kaviyarasu, K.; John Kennedy, L.; Ramalingam, R. J.; Al-Lohedan, H. A. Green Synthesis of NiO Nanoparticles Using Aegle Marmelos Leaf Extract for the Evaluation of In-Vitro Cytotoxicity, Antibacterial and Photocatalytic Properties. *J. Photochem. Photobiol. B Biol.*, **2018**, 180, 39–50.
- [35] Minatel, I. O.; Borges, C. V.; Borges, C. V.; Alonzo, H.; Hector, G.; Gomez, G.; Chen, C. O.; Chen, C. O.; Pace, G.; Lima, P. Phenolic Compounds: Functional Properties, Impact of Processing and Bioavailability, Phenolic Compounds - Biological Activity. *Open Sci.*, **2017**, 1–24.
- [36] Kurek, J. Introductory Chapter: Alkaloids - Their Importance in Nature and for Human Life. *Alkaloids - Their Importance Nat. Hum. Life*, **2019**, 1–7.
- [37] Kregiel, D.; Berlowska, J.; Witonska, I.; Antolak, H.; Proestos, C.; Babic, M.; Babic, L.; Zhang, B. Saponin-Based, Biological-Active Surfactants from Plants. *Appl. Charact. Surfactants*, **2017**.
- [38] Ruiz-Cruz, S.; Chaparro-Hernández, S.; Ruiz, K. L. H.; Cira-Chávez, L. A.; Estrada-Alvarado, M. I.; Ortega, L. E. G.; Ornelas-Paz, J. de J.; Mata, M. A. L. Flavonoids: Important Biocompounds in Food. *Flavonoids - From Biosynth. to Hum. Heal.*, **2017**.

- [39] Kalaichelvi, K. Screening of Phytoconstituents , UV-VIS Spectrum and FT-IR Analysis of *Micrococca Mercurialis* ( L .) Benth. **2017**, 5, 40–44.
- [40] Delgado, A.; Corni, S.; Goldoni, G.; Delgado, A.; Corni, S.; Goldoni, G. Modeling Opto-Electronic Properties of a Dye Molecule in Proximity of a Semiconductor Nanoparticle Modeling Opto-Electronic Properties of a Dye Molecule in Proximity of a Semiconductor Nanoparticle. **2013**, *024105*, 0–11.
- [41] Ansilin, S.; Nair, J. K.; Aswathy, C.; Rama, V.; Peter, J.; Persis, J. J.; Tucker, S.; Autonomous, C. Green Synthesis and Characterisation of Copper Oxide Nanoparticles Using *Azadirachta Indica* ( Neem ) Leaf Aqueous Extract. **2016**, 2, 221–223.
- [42] Baudot, C.; Ming, C.; Chien, J. Infrared Physics & Technology FT-IR Spectroscopy as a Tool for Nano-Material Characterization. *Infrared Phys. Technol.*, **2010**, 53, 434–438.
- [43] Voloshin, Y.; Belaya, I.; Krämer, R. *The Encapsulation Phenomenon*; **2016**.
- [44] Press, D. One-Step Green Synthesis and Characterization of Leaf Extract-Mediated Biocompatible Silver and Gold Nanoparticles from *Memecylon Umbellatum*. **2013**, 1307–1315.
- [45] Birkholz, M. A Practical Guide to X-Ray Crystallography of Biomacro- Molecules Surface and Thin Film Analysis Electron Accelerators as X-Ray Sources Microscopic X-Ray Fluorescence Analysis X-Ray Spectrometry X-Ray Characterization of Materials. **2006**.
- [46] Affam, A. C.; Chaudhuri, M. Degradation of Pesticides Chlorpyrifos , Cypermethrin and Chlorothalonil in Aqueous Solution by TiO<sub>2</sub> Photocatalysis. *J. Environ. Manage.*, **2013**, 130, 160–165.
- [47] Liu, J. Scanning Transmission Electron Microscopy and Its Application to the Study of Nanoparticles and Nanoparticle Systems. **2005**, 54, 251–278.
- [48] Khan, S. A.; Shahid, S.; Ayaz, A.; Alkahtani, J.; Elshikh, M. S.; Riaz, T. Phytomolecules-Coated NiO Nanoparticles Synthesis Using *Abutilon Indicum* Leaf Extract: Antioxidant, Antibacterial, and Anticancer Activities. *Int. J. Nanomedicine*, **2021**, 16, 1757–1773.
- [49] Sharma, S. K.; Verma, D. S.; Khan, L. U.; Kumar, S.; Khan, S. B. *Handbook of Materials Characterization*.
- [50] Kandisa, R. V.; Kv, N. S.; Shaik, K. B.; Gopinath, R. Bioremediation & Biodegradation Dye Removal by Adsorption : A Review. **2016**, 7.
- [51] Enemali, M. O.; Udedi, S. C. Comparative Evaluation of the Protective Effect of Leaf Extracts of *Vernonia Amygdalina* ( Bitter Leaf ) and *Ocimum Canum* ( Curry ) on Acetaminophen Induced Acute Liver Toxicity. **2018**, 10, 116–125.
- [52] Chokkareddy, R.; Redhi, G. Green Synthesis of Metal Nanoparticles and Its Reaction Mechanisms. **2018**.



- [53] Activities, A.; Khan, S. A.; Shahid, S.; Shahid, B.; Fatima, U. Green Synthesis of MnO Nanoparticles Using Abutilon Indicum Leaf Extract for Biological activities . **2020**.
- [54] Das, N.; Ojha, N.; Mandal, S. K. Wastewater Treatment Using Plant-Derived Biofloculants: Green Chemistry Approach for Safe Environment. *Water Sci. Technol.*, **2021**, *83* (8), 1797–1812.
- [55] Rahman, N.; Dewi, N. U. Research Article Phytochemical and Antioxidant Activity of Avocado Leaf Extract ( Persea Americana Mill ).
- [56] Bektas, B.; Gu, K. Journal of Food Composition and Analysis A Novel Hydrogen Peroxide Scavenging Assay of Phenolics and Flavonoids Using Cupric Reducing Antioxidant Capacity ( CUPRAC ) Methodology. **2010**, *23*, 689–698..
- [57] He, W.; Zhou, Y. T.; Wamer, W. G.; Hu, X.; Wu, X.; Zheng, Z.; Boudreau, M. D.; Yin, J. J. Intrinsic Catalytic Activity of Au Nanoparticles with Respect to Hydrogen Peroxide Decomposition and Superoxide Scavenging. *Biomaterials*, **2013**, *34*, 765–773.
- [58] Uddin, S.; Safdar, L. Bin; Anwar, S.; Iqbal, J.; Laila, S.; Abbasi, B. A.; Saif, M. S.; Ali, M.; Rehman, A.; Basit, A.; et al. Green Synthesis of Nickel Oxide Nanoparticles from Berberis Balochistanica Stem for Investigating Bioactivities. **2021**, 1–14.
- [59] Ezhilarasi, A. A.; Vijaya, J. J.; Kaviyarasu, K.; Zhang, X.; Kennedy, L. J. Green Synthesis of Nickel Oxide Nanoparticles Using Solanum Trilobatum Extract for Cytotoxicity, Antibacterial and Photocatalytic Studies. *Surfaces and Interfaces*, **2020**, 100553.
- [60] Gebreslassie, H. B.; Eyasu, A. Phytochemical Screening of the Leaves Calpurnia Aurea ( Ait .) Benth Extract. **2019**, *5*, 18–24.
- [61] Journals, H. Phytochemical Screening of Different Solvent Extracts of Soap Berry ( Phytolacca Dodecandra L ' Herit .) - A Native Ethiopian Shrub. **2016**. 2.
- [62] Rana, P. S. Synthesis , Characterization and Sunlight Catalytic Performance of Cu Doped NiO Nanoparticles. **2019**, 020035.
- [63] Patil, S. Rajiv, P. Sivaraj, R. An investigation of antioxidant and cytotoxic properties of green synthesized silver nanoparticles. *Indo Am. J. Pharm. Sci*, **2015**, 2.
- [64] Abbasi, B. A.; Iqbal, J.; Mahmood, T.; Ahmad, R.; Kanwal, S. Plant-Mediated Synthesis of Nickel Oxide Nanoparticles ( NiO ) via Geranium Wallichianum : Characterization and Different Biological Applications Plant-Mediated Synthesis of Nickel Oxide Nanoparticles ( NiO ) via Geranium Wallichianum : Characterization A. **2019**.
- [65] Khan, S. A.; Shahid, S.; Ayaz, A.; Alkahtani, J.; Elshikh, M. S.; Riaz, T. Phytomolecules-Coated NiO Nanoparticles Synthesis Using Abutilon Indicum Leaf Extract : Antioxidant , Antibacterial , and Anticancer Activities. **2021**, 1757–1773.
- [66] Rajendaran, K.; Muthuramalingam, R.; Ayyadurai, S. Green Synthesis of Ag-Mo/CuO

- Nanoparticles Using Azadirachta Indica Leaf Extracts to Study Its Solar Photocatalytic and Antimicrobial Activities. *Mater. Sci. Semicond. Process.*, **2019**, *91* (September 2018), 230–238.
- [67] Lucas, D. T.; Sica, D. A.; Cássia, R. H.; Luciano, B. M. ST. *Pharm. Dev. Technol.*, **2017**.
- [68] Christopher, J. G.; Saswati, B.; Ezilrani, P. Optimization of Parameters for Biosynthesis of Silver Nanoparticles Using Leaf Extract of Aegle Marmelos. **2015**, *58*, 702–710.
- [69] Loretta, M.; Okalla, C.; Antoinette, A.; Belle, P.; Kedi, E.; Deli, V.; Etoh, M.; Mpondo, E. Spectroscopic Synthetic Optimizations Monitoring of Silver. **2016**.
- [70] Skiba, M. I.; Vorobyova, V. I. Synthesis of Silver Nanoparticles Using Orange Peel Extract Prepared by Plasmochemical Extraction Method and Degradation of Methylene Blue under Solar Irradiation. **2019**, *2019*.
- [71] Adewale, S.; Similoluwa, A.; Adekunle, F.; Kolawole, A. Heliyon Green Synthesis of Copper Oxide Nanoparticles for Biomedical Application and Environmental Remediation. *Heliyon*, **2020**, *6*, 04508.
- [72] Letchumanan, D.; Sok, S. P. M.; Ibrahim, S.; Nagoor, N. H.; Arshad, N. M. Plant-Based Biosynthesis of Copper / Copper Oxide Nanoparticles : An Update on Their Applications in Biomedicine, *Mechanisms and Toxicity*. **2021**.
- [73] Bukhari, S. I.; Hamed, M. M.; Al-agamy, M. H.; Gazwi, H. S. S.; Radwan, H. H.; Youssif, A. M. Biosynthesis of Copper Oxide Nanoparticles Using Streptomyces MHM38 and Its Biological Applications. **2021**.
- [74] Hulkoti, N. I.; Taranath, T. C. Biosynthesis of Nanoparticles Using Microbes-A Review. *Colloids Surfaces B Biointerfaces*, **2014**, *121*, 474–483.
- [75] Chen, M. N.; Chan, C. F.; Huang, S. L.; Lin, Y. S. Green Biosynthesis of Gold Nanoparticles Using Chenopodium Formosanum Shell Extract and Analysis of the Particles' Antibacterial Properties. *J. Sci. Food Agric.*, **2019**, *99*, 3693–3702.
- [76] Upadhyay, L. S. B.; Kumar, N. Green Synthesis of Copper Nanoparticle Using Glucose and Polyvinylpyrrolidone (PVP). *Inorg. Nano-Metal Chem.*, **2017**, *47*, 1436–1440.
- [77] Sheo, L.; Upadhyay, B.; Kumar, N. Green Synthesis of Copper Nanoparticle Using Glucose and Polyvinylpyrrolidone ( PVP ). **2017**, *1556*, 0–22.
- [78] Gnanaprakasam, A.; Sivakumar, V. M.; Thirumarimurugan, M. A Study on Cu and Ag Doped ZnO Nanoparticles for the Photocatalytic Degradation of Brilliant Green Dye : Synthesis and Characterization. **2016**, 1426–1435.
- [79] Varunkumar, K.; Hegde, G.; Ethiraj, A. S. Materials Science in Semiconductor Processing Effect of Calcination Temperature on Cu Doped NiO Nanoparticles Prepared via Wet-Chemical Method : Structural , Optical and Morphological Studies. **2017**, *66*, 149–156.

- [80] Kumar, J. K.; Prasad, A. G. D. Identification and Comparison of Biomolecules in Medicinal Plants of *Tephrosia Tinctoria*. *Rom. J. Biophys.*, **2011**, *21*, 63–71.
- [81] Nomura, K.; Terwilliger, P. Self-Dual Leonard Pairs Aloe Vera Leaf Extract Mediated Green Synthesis of Selenium Nanoparticles and Assessment of Their In Vitro Antimicrobial Activity against Fungi and Pathogenic Bacteria A. **2019**, 399–407.
- [82] Fitokimia, S.; Ekstrak, F.; Daun, M. phytochemical screening and ftir spectroscopy on crude extract from enhalus acoroides leaves. **2020**, *24*, 70–77.
- [83] Vanitha, A.; Kalimuthu, K.; Chinnadurai, V.; Nisha, K. M. J. Phytochemical Screening , FT-IR and GCMS Analysis of Aqueous Extract of *Caralluma Bicolor* – An Endangered Plant. **2019**, *5*, 1122–1130.
- [84] Haq, S.; Dildar, S.; Ali, M. Ben; Mezni, A.; Hed, A.; Shahzad, M. I. Antimicrobial and Antioxidant Properties of Biosynthesized of NiO Nanoparticles Using *Raphanus Sativus* ( *R . Sativus* ) Extract Antimicrobial and Antioxidant Properties of Biosynthesized of NiO Nanoparticles Using *Raphanus Sativus* ( *R . Sativus* ) Extract.
- [85] Academy, C. A.; Town, Y. Phytochemical Screening and Fourier Transform Infrared Spectroscopy ( FT-IR ) Analysis of *Vernonia Amygdalina Del .* ( Bitter Leaf ) Methanol Leaf Extract. **2020**, *14* , 35–41.
- [86] Ramachandran, H.; Jahanara, M. M.; Nair, N. M.; Swaminathan, P. RSC Advances. **2020**, 3951–3959.
- [87] Zahra, T.; Ahmad, K. S. Optik Structural , Optical and Electrochemical Studies of Organo-Templated Wet Synthesis of Cubic Shaped Nickel Oxide Nanoparticles. *Opt. - Int. J. Light Electron Opt.*, **2020**, *205*, 164241.
- [88] Zhang, Q.; Xu, S.; Li, Y.; Ding, P.; Zhang, Y.; Zhao, P. Green-Synthesized Nickel Oxide Nanoparticles Enhances Biohydrogen Production of *Klebsiella Sp .* WL1316 Using Lignocellulosic Hydrolysate and Its Regulatory Mechanism. *Fuel*, **2021**, *305*, 121585.
- [89] Said, A. E. A.; El-wahab, M. M. A.; Soliman, S. A.; Goda, M. N. Synthesis and Characterization of Nano CuO-NiO Mixed Oxides. **2014**, *2*, 17–28.
- [90] Sayyadi, K.; Gharani, M.; Rahdar, A. The Effect of Solvent and Temperature on the Optical and Structural Properties of the Nickel Oxide and Cu-Doped Nickel Oxide Nanoparticles. **2019**, 34–40.
- [91] Ghazal, S.; Khandannasab, N.; Ali, H.; Sabouri, Z.; Rangrazi, A.; Darroudi, M. Green Synthesis of Copper-Doped Nickel Oxide Nanoparticles Using Okra Plant Extract for the Evaluation of Their Cytotoxicity and Photocatalytic Properties. *Ceram. Int.*, **2021**, *47*, 27165–27176.
- [92] Hameeda, B.; Mushtaq, A.; Saeed, M.; Munir, A.; Waseem, A. Development of Cu-Doped NiO

- Nanoscale Material as Efficient Photocatalyst for Visible Light Dye Degradation. *Toxin Rev.*, **2020**, 1–11.
- [93] Karthikeyan, M.; Kumar, P. V.; Ahamed, A. J.; Ravikumar, A. Synthesis of Mg<sup>2+</sup> Doped NiO Nanoparticles and Their Structural and Optical Properties by Co-Precipitation Method. *J. Adv. Appl. Sci. Res.*, **2020**, *1*, 1–9.
- [94] Agale, A. A.; Gaikwad, S. T.; Rajbhoj, A. S. Nanosized Synthesis of Nickel Oxide by Electrochemical Reduction Method and Their Antifungal Screening. *J. Clust. Sci.*, **2017**, *28*, 2097–2109.
- [95] Ezhilarasi, A. A.; Vijaya, J. J.; Kaviyarasu, K.; Kennedy, L. J.; Ramalingam, R. J.; Al-lohedan, H. A. Journal of Photochemistry & Photobiology , B : Biology Green Synthesis of NiO Nanoparticles Using Aegle Marmelos Leaf Extract for the Evaluation of in-Vitro Cytotoxicity , Antibacterial and Photocatalytic Properties. *J. Photochem. Photobiol. B Biol.*, **2018**, *180*, 39–50.
- [96] Khalil, A. T.; Ovais, M.; Ullah, I.; Ali, M.; Khan, Z.; Maaza, M.; Talha, A.; Ovais, M.; Ullah, I.; Ali, M. Green Chemistry Letters and Reviews Biosynthesis of Iron Oxide ( Fe<sub>2</sub>O<sub>3</sub> ) Nanoparticles via Aqueous Extracts of Sageretia Thea ( Osbeck .) and Their Pharmacognostic Properties. *Green Chem. Lett. Rev.*, **2017**, *10*, 186–201.
- [97] Iteku, J. B.; Mbayi, O.; Bongo, G. N.; Mutwale, P. K.; Wambale, J. M.; Lengbiye, E.; Inkoto, C. L.; Ngunde, S. N.; Ngbolua, K. Phytochemical Analysis and Assessment of Antibacterial and Antioxidant Activities of Phytolacca Dodecandra L . Herit Leaf Extracts ( Phytolaccaceae ). **2019**, *5*, 31–39.
- [98] Umar, H.; Kava, D.; Rizaner, N. Biosynthesis of Zinc Oxide Nanoparticles Using Albizia Lebbeck Stem Bark , and Evaluation of Its Antimicrobial , Antioxidant , and Cytotoxic Activities on Human Breast Cancer Cell Lines. **2019**, 87–100.

## APPENDIX

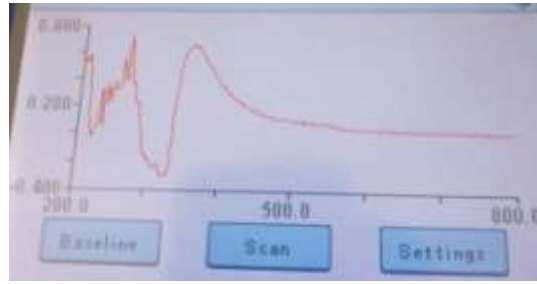


Figure 30. UV-Vis absorbance of plant extract.

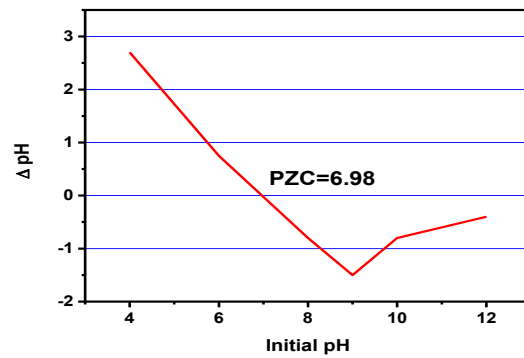


Figure 31. PZC OF Cu-NiO

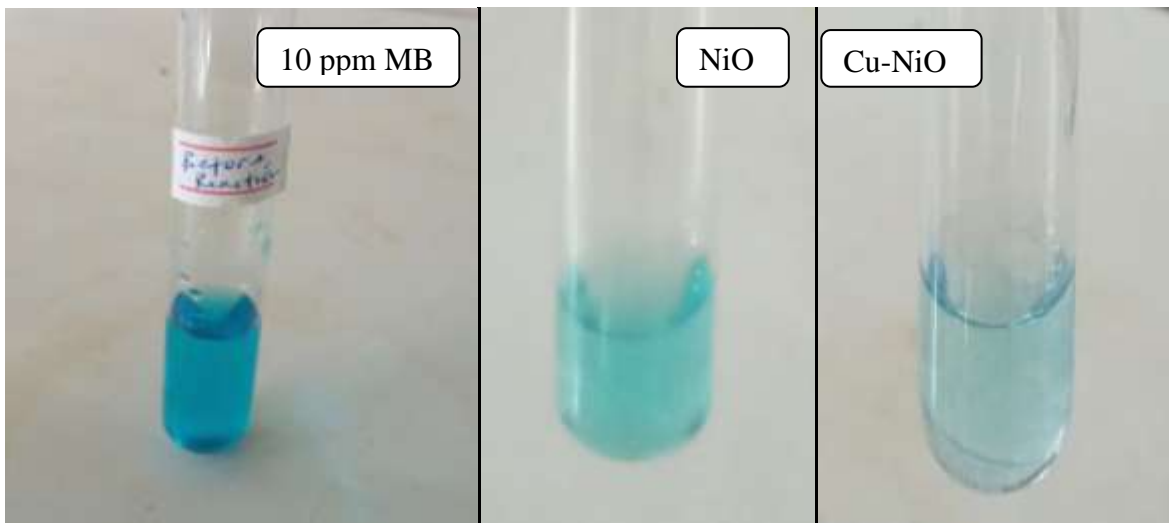


Figure 32. Methylene blue before and after photocatalytically degraded.



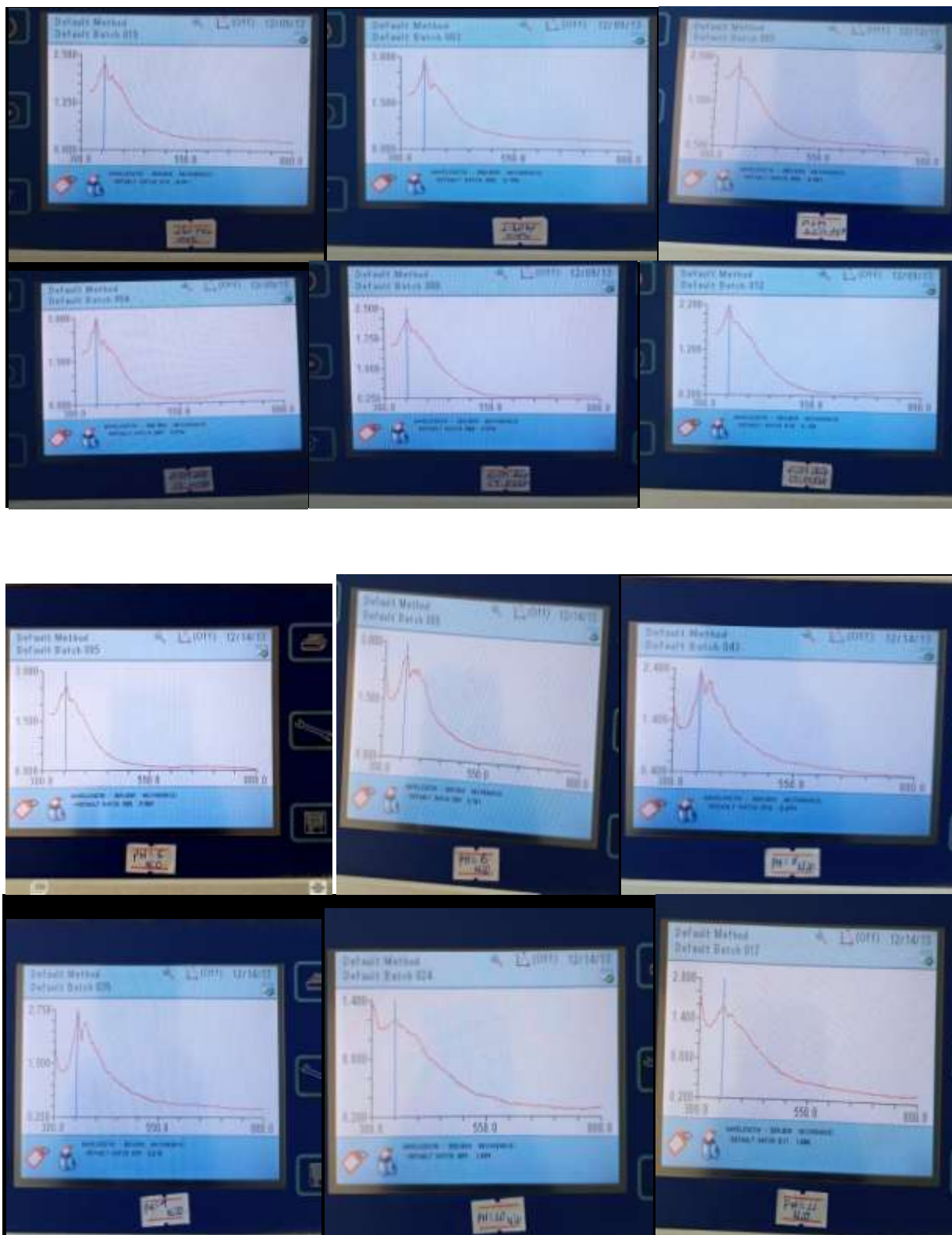


Figure 33. Optimization of different parameters of synthesizes.